Molecular Cell, Volume *81*

Supplemental information

AHNAK controls 53BP1-mediated p53 response by restraining 53BP1 oligomerization and phase separation

Indrajeet Ghodke, Michaela Remisova, Audrey Furst, Sinan Kilic, Bernardo Reina-San-Martin, Anna R. Poetsch, Matthias Altmeyer, and Evi Soutoglou

Figure-S1

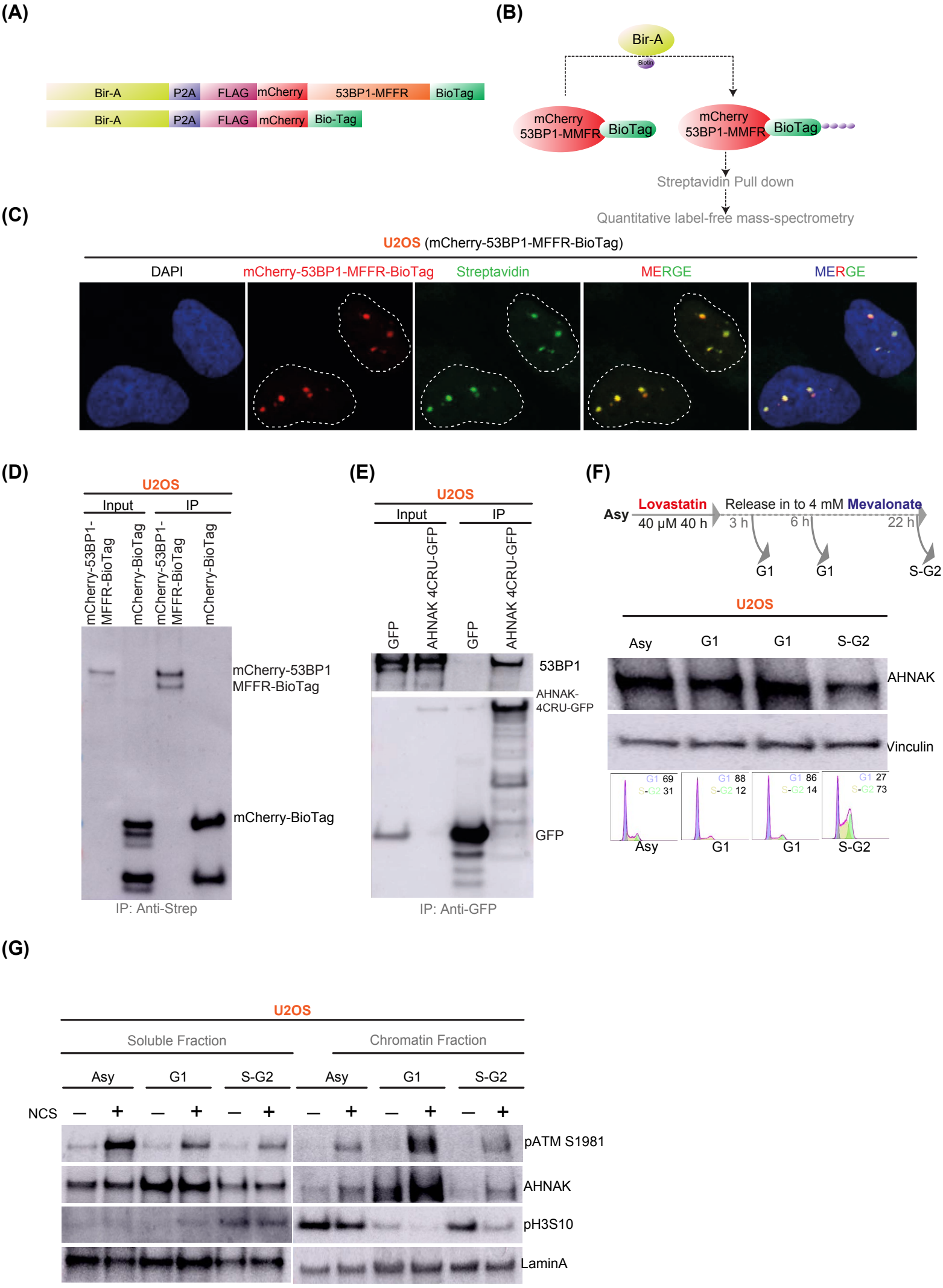
(A)
Bir-A
P2A
FLAG
mCherry
53BP1-MFFR
BioTag
Bir-A
P2A
FLAG
mCherry
Bio-Tag
(B)
Bir-A
Biotin
mCherry
53BP1-MMFR
BioTag
mCherry
53BP1-MMFR
BioTag
Streptavidin Pull down
Quantitative label-free mass-spectrometry
(C)
U2OS (mCherry-53BP1-MFFR-BioTag)
DAPI
mCherry-53BP1-MFFR-BioTag
Streptavidin
MERGE
MERGE
(D)
U2OS
Input
IP
mCherry-53BP1-MFFR-BioTag
mCherry-BioTag
mCherry-53BP1-MFFR-BioTag
mCherry-BioTag
mCherry-53BP1 MFFR-BioTag
mCherry-BioTag
IP: Anti-Strep
(E)
U2OS
Input
IP
GFP
AHNAK 4CRU-GFP
GFP
AHNAK 4CRU-GFP
53BP1
AHNAK-4CRU-GFP
GFP
IP: Anti-GFP
(F)
Asy
Lovastatin
40 μM 40 h
Release in to 4 mM Mevalonate
3 h
6 h
22 h
G1
G1
S-G2
U2OS
Asy
G1
G1
S-G2
AHNAK
Vinculin
G1 69
S-G2 31
G1 88
S-G2 12
G1 86
S-G2 14
G1 27
S-G2 73
Asy
G1
G1
S-G2
(G)
U2OS
Soluble Fraction
Chromatin Fraction
Asy
G1
S-G2
Asy
G1
S-G2
NCS
– + – + – + – + – + – +
pATM S1981
AHNAK
pH3S10
LaminA

Figure-S2

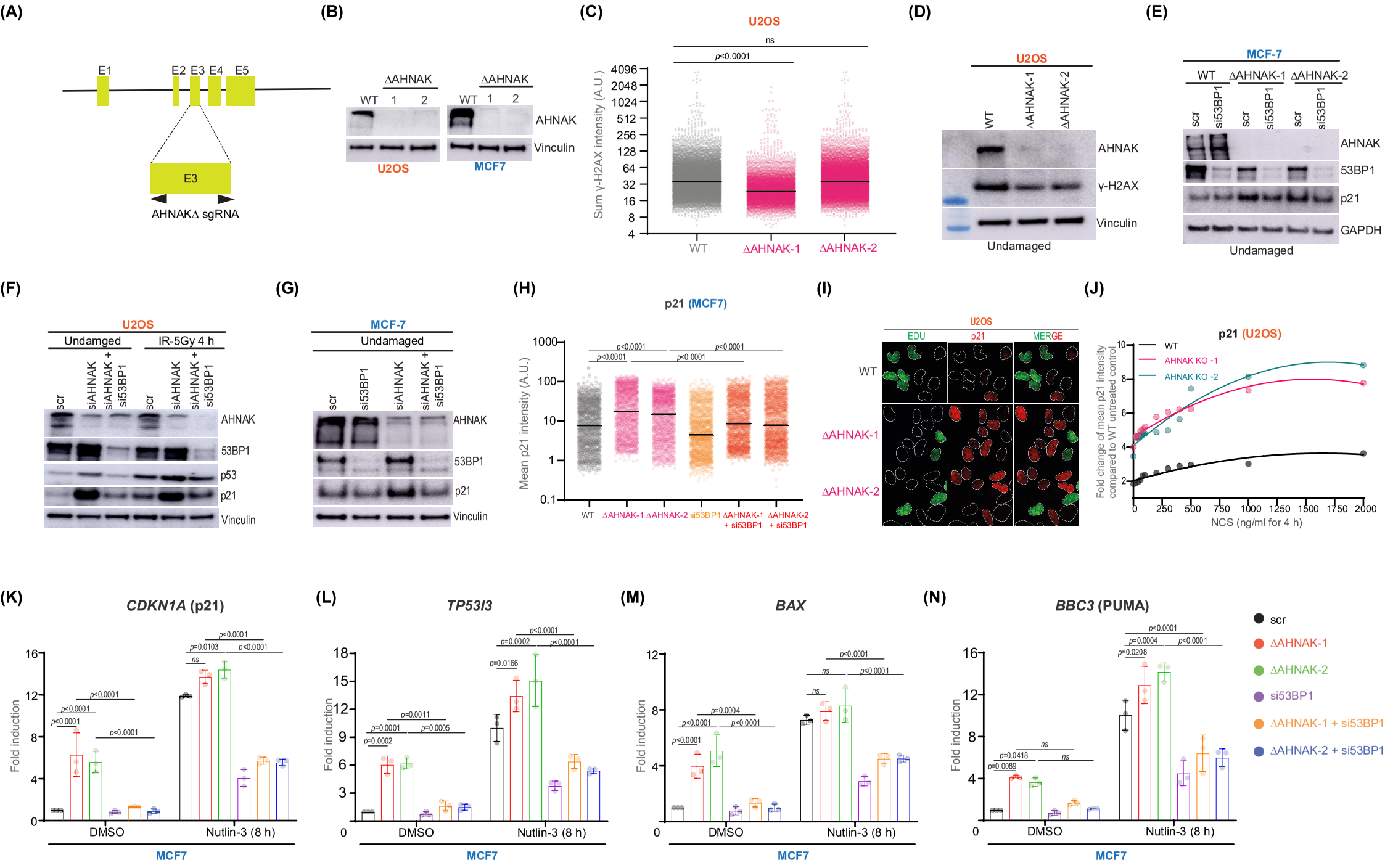
(A)
E1
E2 E3 E4 E5
E3
AHNAKΔ sgRNA
(B)
ΔAHNAK
WT 1 2
ΔAHNAK
WT 1 2
AHNAK
Vinculin
U2OS
MCF7
(C)
U2OS
ns
p<0.0001
Sum γ-H2AX intensity (A.U.)
4096
2048
1024
512
256
128
64
32
16
8
4
WT
ΔAHNAK-1
ΔAHNAK-2
(D)
U2OS
WT
ΔAHNAK-1
ΔAHNAK-2
AHNAK
γ-H2AX
Vinculin
Undamaged
(E)
MCF-7
WT
ΔAHNAK-1
ΔAHNAK-2
scr
si53BP1
AHNAK
53BP1
p21
GAPDH
Undamaged
(F)
U2OS
Undamged
IR-5Gy 4 h
scr
siAHNAK
siAHNAK + si53BP1
AHNAK
53BP1
p53
p21
Vinculin
(G)
MCF-7
Undamaged
scr
si53BP1
siAHNAK
siAHNAK + si53BP1
AHNAK
53BP1
p21
Vinculin
(H)
p21 (MCF7)
Mean p21 intensity (A.U.)
1000
100
10
1
0.1
p<0.0001
WT
ΔAHNAK-1
ΔAHNAK-2
si53BP1
ΔAHNAK-1 + si53BP1
ΔAHNAK-2 + si53BP1
(I)
U2OS
EDU
p21
MERGE
WT
ΔAHNAK-1
ΔAHNAK-2
(J)
p21 (U2OS)
Fold change of mean p21 intensity compared to WT untreated control
WT
AHNAK KO -1
AHNAK KO -2
NCS (ng/ml for 4 h)
0
250
500
750
1000
1250
1500
1750
2000
(K)
CDKN1A (p21)
Fold induction
DMSO
Nutlin-3 (8 h)
MCF7
(L)
TP53I3
Fold induction
DMSO
Nutlin-3 (8 h)
MCF7
(M)
BAX
Fold induction
DMSO
Nutlin-3 (8 h)
MCF7
(N)
BBC3 (PUMA)
Fold induction
DMSO
Nutlin-3 (8 h)
MCF7
scr
ΔAHNAK-1
ΔAHNAK-2
si53BP1
ΔAHNAK-1 + si53BP1
ΔAHNAK-2 + si53BP1

Figure-S3

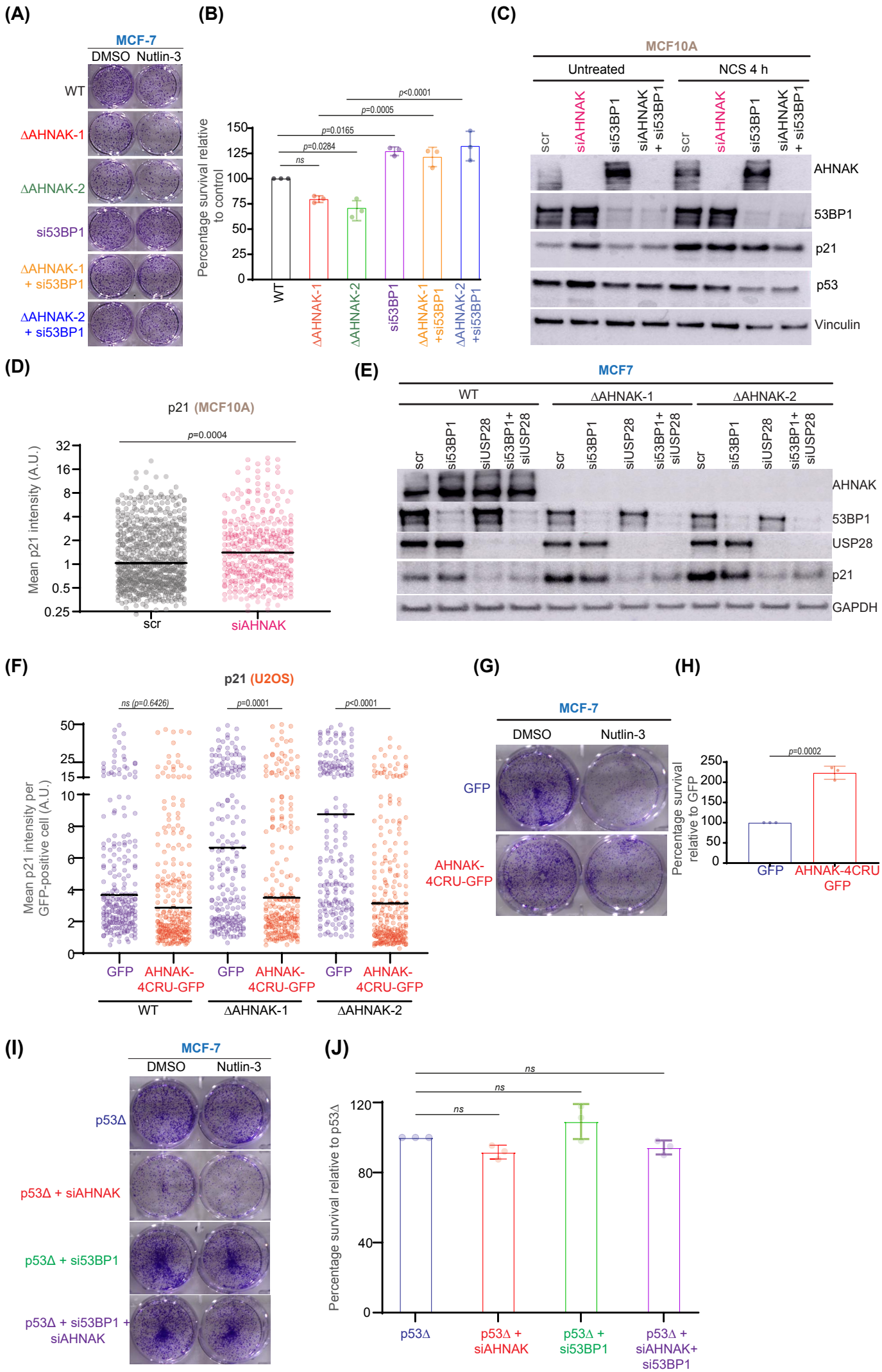
(A)
MCF-7
DMSO Nutlin-3
WT
ΔAHNAK-1
ΔAHNAK-2
si53BP1
ΔAHNAK-1 + si53BP1
ΔAHNAK-2 + si53BP1
(B)
Percentage survival relative to control
p<0.0001
p=0.0005
p=0.0165
p=0.0284
ns
WT
ΔAHNAK-1
ΔAHNAK-2
si53BP1
ΔAHNAK-1 +si53BP1
ΔAHNAK-2 +si53BP1
(C)
MCF10A
Untreated
NCS 4 h
scr
siAHNAK
si53BP1
siAHNAK + si53BP1
AHNAK
53BP1
p21
p53
Vinculin
(D)
p21 (MCF10A)
p=0.0004
Mean p21 intensity (A.U.)
scr
siAHNAK
(E)
MCF7
WT
ΔAHNAK-1
ΔAHNAK-2
scr
si53BP1
siUSP28
si53BP1+ siUSP28
AHNAK
53BP1
USP28
p21
GAPDH
(F)
p21 (U2OS)
ns (p=0.6426)
p=0.0001
p<0.0001
Mean p21 intensity per GFP-positive cell (A.U.)
GFP
AHNAK-4CRU-GFP
WT
ΔAHNAK-1
ΔAHNAK-2
(G)
MCF-7
DMSO
Nutlin-3
GFP
AHNAK-4CRU-GFP
(H)
p=0.0002
Percentage survival relative to GFP
GFP
AHNAK-4CRU GFP
(I)
MCF-7
DMSO
Nutlin-3
p53Δ
p53Δ + siAHNAK
p53Δ + si53BP1
p53Δ + si53BP1 + siAHNAK
(J)
ns
ns
ns
Percentage survival relative to p53Δ
p53Δ
p53Δ + siAHNAK
p53Δ + si53BP1
p53Δ + siAHNAK+ si53BP1

Figure-S4

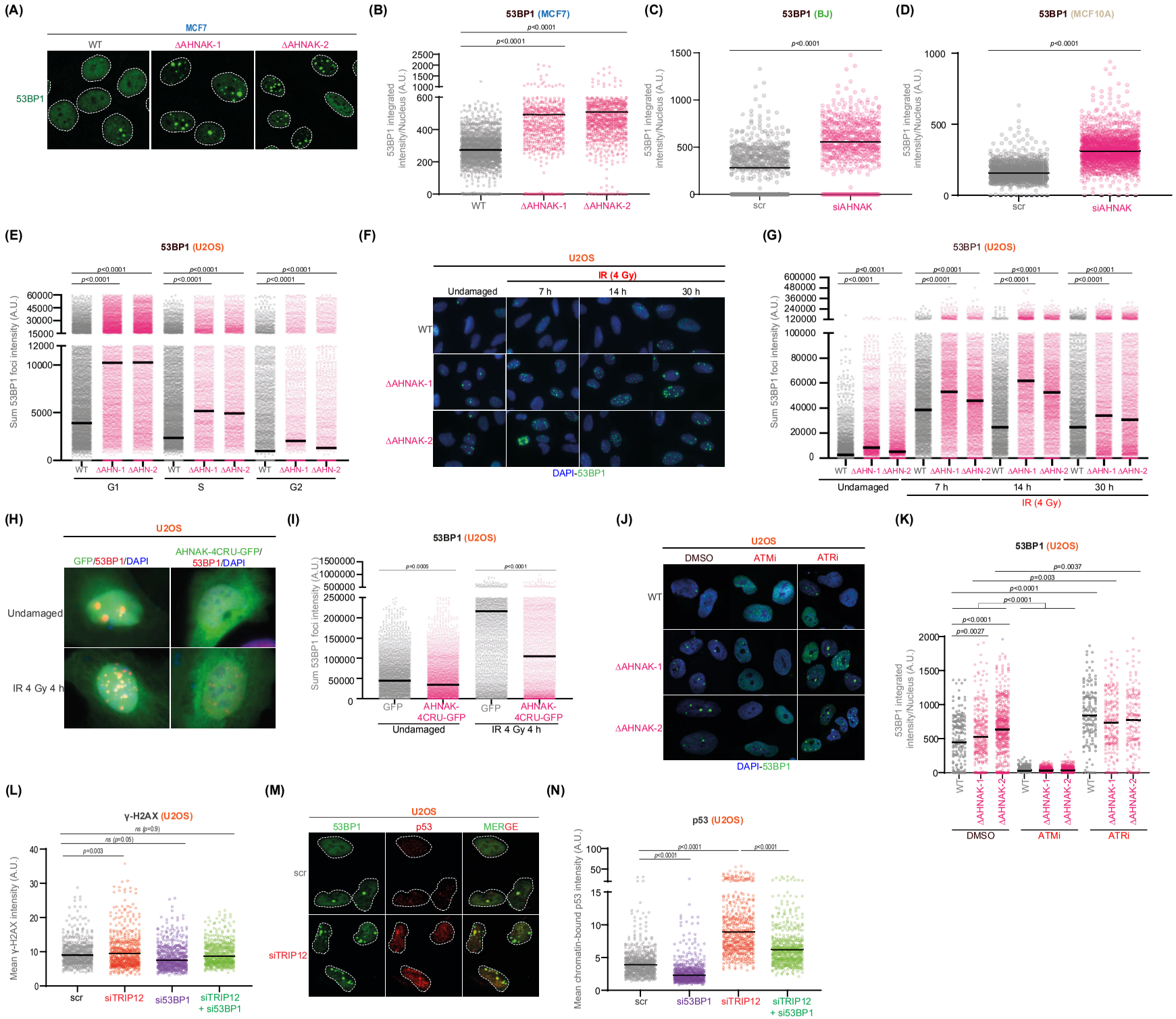
(A)
MCF7
WT
ΔAHNAK-1
ΔAHNAK-2
53BP1
(B)
53BP1 (MCF7)
p<0.0001
53BP1 integrated intensity/Nucleus (A.U.)
WT
ΔAHNAK-1
ΔAHNAK-2
(C)
53BP1 (BJ)
p<0.0001
scr
siAHNAK
(D)
53BP1 (MCF10A)
p<0.0001
scr
siAHNAK
(E)
53BP1 (U2OS)
Sum 53BP1 foci intensity (A.U.)
WT ΔAHN-1 ΔAHN-2
G1
S
G2
(F)
U2OS
IR (4 Gy)
Undamaged
7 h
14 h
30 h
WT
ΔAHNAK-1
ΔAHNAK-2
DAPI-53BP1
(G)
53BP1 (U2OS)
Sum 53BP1 foci intensity (A.U.)
Undamaged
7 h
14 h
30 h
IR (4 Gy)
(H)
U2OS
GFP/53BP1/DAPI
AHNAK-4CRU-GFP/53BP1/DAPI
Undamaged
IR 4 Gy 4 h
(I)
53BP1 (U2OS)
Sum 53BP1 foci intensity (A.U.)
GFP
AHNAK-4CRU-GFP
Undamaged
IR 4 Gy 4 h
(J)
U2OS
DMSO
ATMi
ATRi
WT
ΔAHNAK-1
ΔAHNAK-2
DAPI-53BP1
(K)
53BP1 (U2OS)
53BP1 integrated intensity/Nucleus (A.U.)
DMSO
ATMi
ATRi
(L)
γ-H2AX (U2OS)
Mean γ-H2AX intensity (A.U.)
scr
siTRIP12
si53BP1
siTRIP12 + si53BP1
(M)
U2OS
53BP1
p53
MERGE
scr
siTRIP12
(N)
p53 (U2OS)
Mean chromatin-bound p53 intensity (A.U.)
scr
si53BP1
siTRIP12
siTRIP12 + si53BP1

Figure-S5

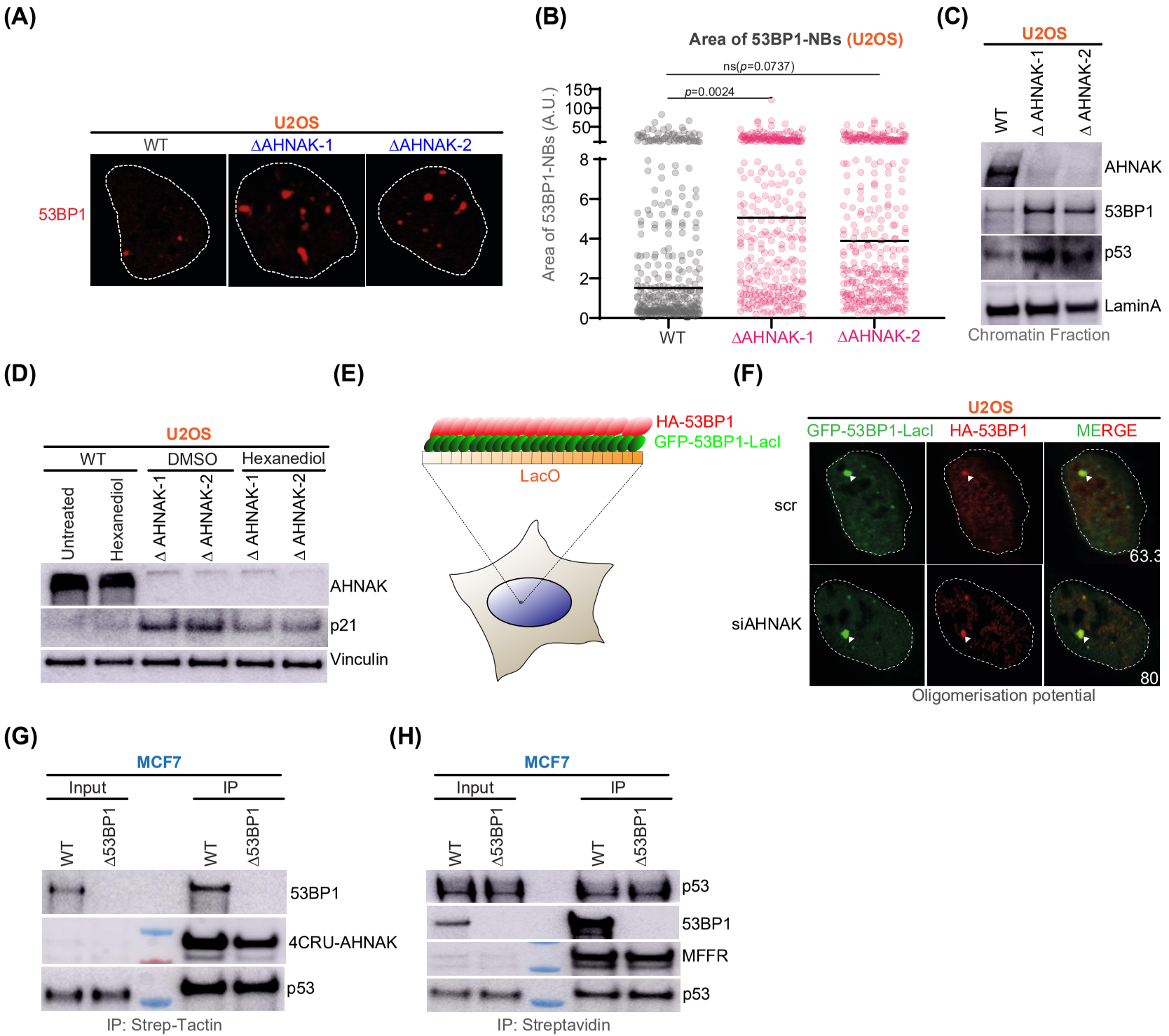
(A)
U2OS
WT
ΔAHNAK-1
ΔAHNAK-2
53BP1
(B)
Area of 53BP1-NBs (U2OS)
ns(p=0.0737)
p=0.0024
Area of 53BP1-NBs (A.U.)
150
100
50
8
6
4
2
0
WT
ΔAHNAK-1
ΔAHNAK-2
(C)
U2OS
WT
Δ AHNAK-1
Δ AHNAK-2
AHNAK
53BP1
p53
LaminA
Chromatin Fraction
(D)
U2OS
WT
DMSO
Hexanediol
Untreated
Hexanediol
Δ AHNAK-1
Δ AHNAK-2
Δ AHNAK-1
Δ AHNAK-2
AHNAK
p21
Vinculin
(E)
HA-53BP1
GFP-53BP1-LacI
LacO
(F)
U2OS
GFP-53BP1-LacI
HA-53BP1
MERGE
scr
siAHNAK
63.3
80
Oligomerisation potential
(G)
MCF7
Input
IP
WT
Δ53BP1
WT
Δ53BP1
53BP1
4CRU-AHNAK
p53
IP: Strep-Tactin
(H)
MCF7
Input
IP
WT
Δ53BP1
WT
Δ53BP1
p53
53BP1
MFFR
p53
IP: Streptavidin

Figure-S6

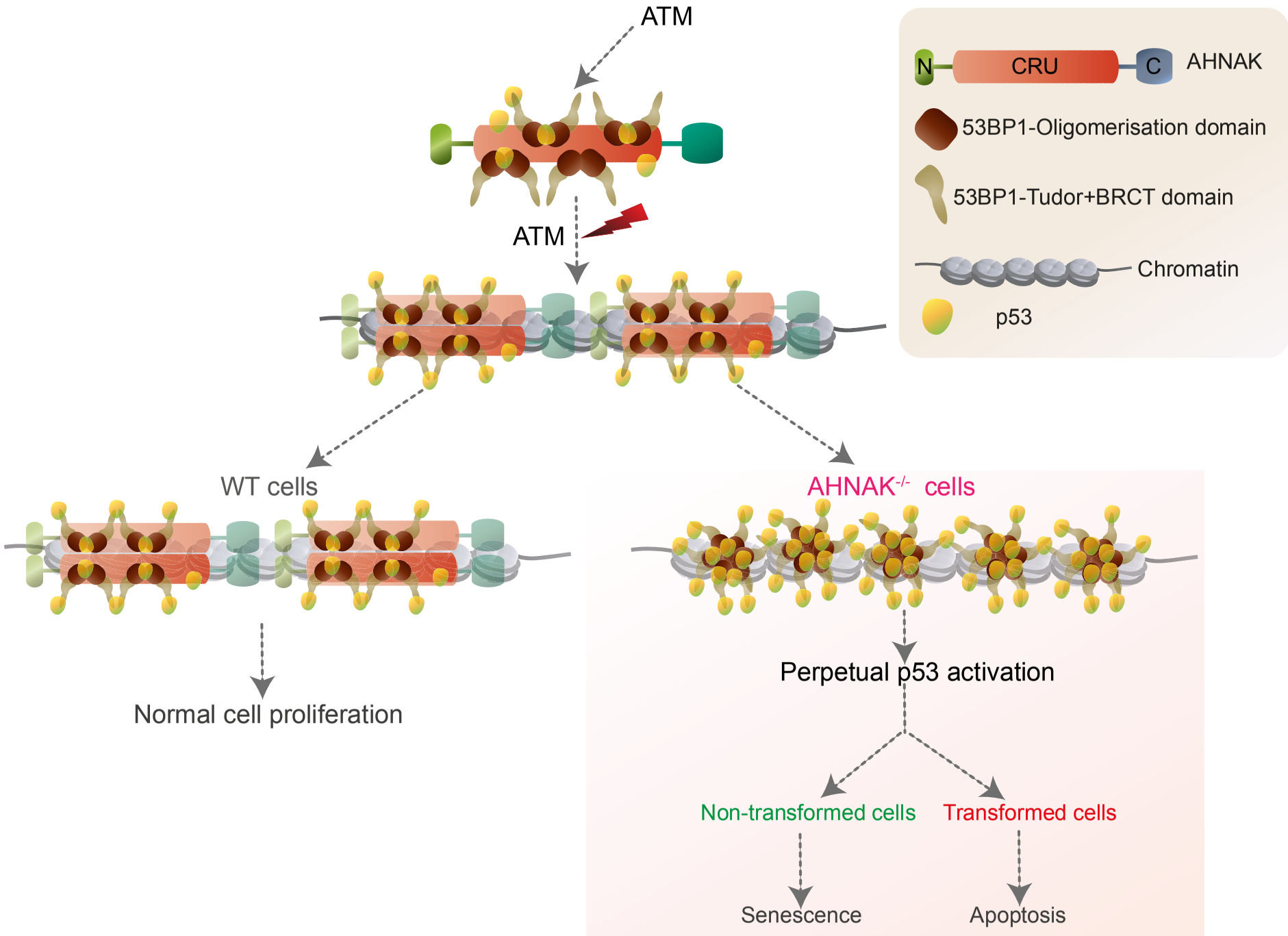
ATM
ATM
N
CRU
C
AHNAK
53BP1-Oligomerisation domain
53BP1-Tudor+BRCT domain
Chromatin
p53
WT cells
AHNAK-/- cells
Normal cell proliferation
Perpetual p53 activation
Non-transformed cells
Transformed cells
Senescence
Apoptosis

SUPPLEMENTARY FIGURE LEGENDS

Figure-S1 (related to main Figure 1)

Characterization of AHNAK-53BP1 interaction

Schematic illustrations of **(A)** constructs, **(B)** *in-vivo* tagging system used in this study. **(C)** Representative confocal image of U2OS cells stably expressing WT-BirA and mCherry-53BP1-MFFR-BioTag and incubated with biotin for 24 h and stained with Streptavidin (fluorescein green) and Dapi (blue). Dashed line delineates the edge of the nucleus. **(D)** U2OS stable cell lines expressing the constructs described in **A** were subjected to immunoprecipitation using Streptavidin beads, and bound complexes were analyzed by immunoblotting using Anti-mCherry antibody. **(E)** U2OS cells transiently transfected with GFP or AHNAK-4CRU-GFP were subjected to immunoprecipitation using GFP trap beads, and bound complexes were analyzed by immunoblotting using Anti-GFP and Anti-53BP1 antibodies. **(F)** Top; Schematic of cell cycle synchronization by lovastatin. Briefly, U2OS cells were synchronized in G1 by 40 μM lovastatin for 40 h and released into the medium containing 4 mM Mevalonolactone. Cell lysates from asynchronous cells or cells synchronized as above were analyzed by immunoblot using the indicated antibodies. Vinculin was used as a loading control. For verification of the cell cycle stage, cells were fixed, stained with propidium iodide and analyzed by flow cytometry as shown in bottom. **(G)** Soluble and insoluble fractions from U2OS cells arrested in G1 following Lovastatin treatment and released in S/G2, were subjected to western blot analysis with the specified antibodies.

Figure-S2 (related to main Figure 2)

AHNAK triggers optimal 53BP1-mediated p53 activity

(A) Schematic illustration of the human AHNAK locus and the positions of gRNAs selected for the generation of AHNAK knockout cell-lines. **(B)** Confirmation of AHNAK knock out by Immunoblot analysis of lysates prepared from the WT and two independent AHNAK $^{-/-}$ U2OS

and MCF7 cell lines using AHNAK antibody. **(C)** WT and two independent AHNAK$^{-/-}$ U2OS cell lines under unperturbed conditions were stained for γ-H2AX, and the nuclear signal intensity was quantified using QIBC. The solid line denotes median. A.U., arbitrary units, ($n \geq$ 8733 cells per condition). **(D)** Immunoblot analysis of Cell lysates prepared from WT and two independent AHNAK $^{-/-}$ U2OS cell lines under unperturbed conditions using the indicated antibodies. Vinculin was used as a loading control. **(E)** Immunoblot analysis of WT and two independent AHNAK $^{-/-}$ MCF7 cell lines following transfection with control or 53BP1 siRNA. Cell lysates were prepared under unperturbed conditions and then analyzed by the indicated antibodies. GAPDH was used as a loading control. **(F)** Immunoblot analysis of U2OS cells transfected with control, AHNAK or 53BP1 siRNAs. Cell lysates were prepared from cells either untreated or exposed to ionization radiation (5 Gy, 4 h recovery). Vinculin was used as a loading control. **(G)** Immunoblot analysis of MCF7 cells transfected with control, AHNAK or 53BP1 siRNAs. Cell lysates were prepared under undamaged conditions. Vinculin was used as a loading control. **(H)** Quantification of p21 fluorescence intensity in WT and two independent AHNAK $^{-/-}$ MCF7 cell lines transfected with scramble or 53BP1 siRNA. The solid line denotes median. A.U., arbitrary units, (n=963). **(I)** Representative confocal images of subcellular localization of p21 (fluorescein green) by co-staining with EDU (red) in WT and two independent AHNAK $^{-/-}$ U2OS cell lines under unperturbed conditions. Dashed line delineates the edge of the nucleus. **(J)** Graphical representation of mean nuclear p21 intensity for dose-dependent titration of NCS (0 to 2000 ng/ml for 4 h) in WT and two independent AHNAK $^{-/-}$ U2OS cell lines (n >1000 cells). Each circle represents median at respective NCS concentration. **(K-N)** qRT-PCR analysis of p53 target genes expression in WT and two independent AHNAK $^{-/-}$ MCF7 cell lines transfected with control or 53BP1 siRNA. Cells were treated with DMSO or Nutlin-3 treated (4 μM 8 h). **(K)** *CDKN1A,* **(L)** *TP53I3,* **(M)** *BAX,* and

(N) *BBC3*. *GAPDH* transcript was used for normalization, before the calculation of fold change.

Figure-S3 (related to main Figure 2)

AHNAK suppresses perpetual p53 activation in both transformed and non-transformed cell lines

(A-B) Effect of Nutlin-3 on the survival of cells. WT and two independent AHNAK $^{-/-}$ MCF7 cell lines transfected with control or siRNA against 53BP1 were treated with 10 μM Nutlin-3 or DMSO for 18 hours. After 7 days, colonies were stained with crystal violet **(A)** and quantified **(B)**. **(C)** MCF10A cells transfected with control or indicated siRNA. Cell lysates from untreated and NCS (100 ng/ml) treated cells, were analyzed by immunoblotting using the indicated antibodies. Vinculin was used as a loading control. **(D)** Quantification of mean nuclear p21 signal fluorescence intensity in individual cells of MCF10A cells transfected with control or AHNAK siRNA under unperturbed conditions. The solid line denotes median. A.U., arbitrary units, ($n \geq 323$, Unpaired t-test). **(E)** Immunoblot analysis of MCF7 cell lines using the indicated antibodies following transfection with control or indicated siRNA under unperturbed conditions. GAPDH was used as a loading control. **(F)** Quantification of p21 fluorescence intensity in GFP positive nuclei of WT and two independent AHNAK $^{-/-}$ U2OS cell lines after transient overexpression with GFP or AHNAK-4CRU-GFP. The solid line denotes median. A.U., arbitrary units, (n=228). **(G-H)** Effect of Nutlin-3 after overexpression of GFP or AHNAK-4CRU-GFP on the survival of MCF7 cells. Cells treated with DMSO or Nutlin-3 (10 μM, 18 h) treated, and after 7 days, colonies were stained with crystal violet **(G)** and quantification **(H). (I-J)** Effect of Nutlin-3 (10 μM, 18 h) on MCF7 p53$^{-/-}$ cells survival after transfection with control or indicated siRNAs. Colonies were stained with crystal violet **(I)** and quantification **(J)**

Figure-S4 (related to main Figure 4)

AHNAK restrains 53BP1 accrual in the chromatin.

(A) Representative confocal images following immunostaining of 53BP1 foci (fluorescein green) in WT and two independent AHNAK $^{-/-}$ MCF7 cell lines under unperturbed conditions. Dashed line delineates the edge of the nucleus. **(B)** Quantification of integrated fluorescence intensity of 53BP1-NBs in individual cells of the indicated genotype of MCF7 cell lines. The solid line denotes median. The solid line denotes median. A.U., arbitrary units, ($n \geq 616$). **(C)** Quantification of integrated fluorescence intensity of 53BP1-NBs in individual cells of BJ transfected with control or AHNAK siRNA under unperturbed conditions. The solid line denotes median. A.U., arbitrary units, ($n \geq 458$, Unpaired t-test). **(D)** Quantification of mean 53BP1 integrated fluorescence intensity in individual cells of MCF10A cells transfected with control or AHNAK siRNA under unperturbed conditions. The solid line denotes median. A.U., arbitrary units, ($n \geq 958$, Unpaired t-test). **(E)** WT and two independent AHNAK$^{-/-}$ U2OS cell lines under unperturbed conditions were stained for 53BP1, and the sum 53BP1 foci intensity was quantified in a cell cycle resolved manner using QIBC. The solid line denotes median. A.U., arbitrary units, ($n \geq 2442$ cells per condition). **(F)** Representative images of WT and two independent AHNAK$^{-/-}$ U2OS cell lines treated with 4 Gy of IR and released for the indicated time points. Cells were stained for 53BP1 (fluorescein green) and DAPI (blue). **(G)** The sum of total 53BP1 foci intensity per cell was quantified from >2000 cells per condition by QIBC. The solid line denotes median. A.U., arbitrary units. **(H)** Representative images of of U2OS cells after transient transfection with GFP or AHNAK-4CRU-GFP in absence and presence of DNA damage by IR (4 Gy 4 h). **(I)** Quantification of sum 53BP1 foci intensity from panel **(H)** The solid line denotes median. A.U., arbitrary units, ($n \geq 3757$ cells per condition)**.** **(J)** Representative images of WT and two independent AHNAK$^{-/-}$ U2OS cell lines pre incubated with 10 μM ATMi (KU 55933) and 5 μM ATRi (AZD 6738) for 1 h and immunostained with

53BP1. Dashed line delineates the edge of the nucleus. **(K)** Quantification of integrated fluorescence intensity of 53BP1-NBs in individual cells as in **(J)**. The solid line denotes median. A.U., arbitrary units, ($n \geq 152$). **(L)** Quantification of mean γ-H2AX nuclear fluorescence intensity in individual cells after indicated siRNA-mediated depletion in U2OS cells. The solid line denotes median. A.U., arbitrary units, ($n \geq 851$). **(M)** Representative confocal images after pre-extraction of soluble protein in U2OS cells co-immunostained for 53BP1 (fluorescein green) and p53 (red) after indicated siRNA-mediated depletion. Dashed line delineates the edge of the nucleus. **(N)** Quantification of mean chromatin-bound p53 fluorescence intensity in individual cells after indicated siRNA-mediated depletion after pre-extraction in U2OS cells. The solid line denotes median. A.U., arbitrary units, (n=429).

Figure-S5. (related to main Figure 5)

Enhanced 53BP1 phase-separation in absence of AHNAK is responsible for mounting p53 response

(A) Representative confocal images following immunostaining of 53BP1 foci (fluorescein green) in WT and two independent AHNAK$^{-/-}$ U2OS cell lines under unperturbed conditions. Dashed line delineates the edge of the nucleus. **(B)** Quantification of the area of 53BP1-NBs in WT and two independent AHNAK $^{-/-}$ U2OS cell lines. The solid line indicates the median. A.U., arbitrary units, (n=297 53BP1-NBs). **(C)** Immunoblot analysis of chromatin fractions from WT and two independent AHNAK$^{-/-}$ U2OS cell lines. LaminA was used as a loading control for chromatin fractions. **(D)** Following DMSO or 1,6-hexanediol (1% for 4 h) treatment of WT and two independent AHNAK$^{-/-}$ U2OS cell lines, cell lysates were subjected to western blot analysis with indicated antibodies. Vinculin was used as a loading control. **(E)** Schematic illustration of the tethering system. **(F)** Co-localization of GFP-LacI-53BP1 with HA-53BP1(red) on the LacO array in U2OS19 cells after transfection with indicated siRNA. The

white numbers represent % of cells which exert colocalization of the indicated protein with the lacO array. **(G)** WT MCF7 and Δ53BP1-MCF7 cells were transiently transfected with strep tagged AHNAK-4CRU plasmid. After pulldown with Strep-Tactin beads, co-precipitated 53BP1 and p53 were detected by immunoblotting as indicated. **(H)** WT MCF7 and Δ53BP1-MCF7 cells under unperturbed conditions were transiently transfected with mCherry-53BP1 MFFR-BioTag. After pulldown with streptavidin beads, co-precipitated AHNAK and p53 were detected by immunoblotting as indicated.

Figure-S6

Model depicting AHNAK involvement in optimizing p53 responses by restraining 53BP1 phase separation

Table S1 (Related to STAR Methods)

Primers for cloning

Primers for plasmid constructions	Forward Primer	Reverse Primer
53BP1-Tudor (1271-1771 aa)	CGAATGCATCTAGATATCGGATCCCGGTCTCGGAACATGGAGGAGACTGAAGAGCCAATTGTAGAGTG	GCAGGCCTCTGCAGTCGACGGGCCCGGTCTCTTGCTCCTTCACCGGTGTTGTCTCCACTCTCACAGGGGC
53BP1-MFFR (1220-1771 aa)	CGAATGCATCTAGATATCGGATCCCGGTCTCGGAACATGCAGGGAGAAGAAGAG	GCAGGCCTCTGCAGTCGACGGGCCCGGTCTCTTGCTCCTTCACCGGTGTTGTCTCCA
53BP1-MFFR-BRCT (1220-1972 aa)	CGAATGCATCTAGATATCGGATCCCGGTCTCGGAACATGCAGGGAGAAGAAGAGTTTGATATGCCTCAG	GCAGGCCTCTGCAGTCGACGGGCCCGGTCTCTTGCTCCGTGAGAAACATAATCGTGTTTATATTTTGGA

Table S2 (Related to STAR Methods)

Sequence of CRISPR-Cas9 guide-RNAs (gRNAs) and primer pairs used to generate AHNAK knockout in all the cell lines used in this study.

gRNA for KO	Sequence	Forward Primer	Reverse Primer
AHNAK-pGH-212	AGAACAGAGCTCTAGTCATG	AAAGAAGACAAACCTAGAACAGAGCTCTAGTCATGGTTTAAGTCTTCTTT	AAAGAAGACTTAAACCATGACTAGAGCTCTGTTCTAGGTTTGTCTTCTTT
AHNAK-pGH-213	AGGGCCCAGTCATTATCCTG	AAAGAAGACAAACCTAGGGCCCAGTCATTATCCTGGTTTAAGTCTTCTTT	AAAGAAGACTTAAACCAGGATAATGACTGGGCCCTAGGTTTGTCTTCTTT

Table S3 (Related to STAR Methods)

Sequences of primer pairs used for RT-qPCR in this study.

Primers for qPCR	**Forward Primer**	**Reverse Primer**
CDKN1A (p21)	CCTCATCCCGTGTTCTCCTTT	GTACCACCCAGCGGACAAGT
BAX	CCTTTTCTACTTTGCCAGCAAAC	GAGGCCGTCCCAACCAC
BBC3 (PUMA)	CCTGGAGGGTCCTGTACAATCT	GCACCTAATTGGGCTCCATCT
TP53I3	AGGGTGAAGTCCTCCTGAAGGT	GTGGGTCATACTGGCCTTGTCT
AHNAK	ATGCTCCAGGGCTCAACCT	CGTGCCCCAACGTTAAGCTT
TP53BP1	CTCTGCCCATGCCTCACAA	ACCTCCCAGCACTGACAATA
GAPDH	CGAAGTTGGTGTAGGGTTTGACT	AGGTCGGTGTGAACGGATTTG
β-ACTIN	CGCGAGAAGATGACCCAGA	GGGCATACCCCTCGTAGAT

Data S1 Uncropped WB images
(Related to Figure 1, 2, 4, 5, S1, S2, S3 and S5)

(Related to Figure 1)

Related to Figure 1C

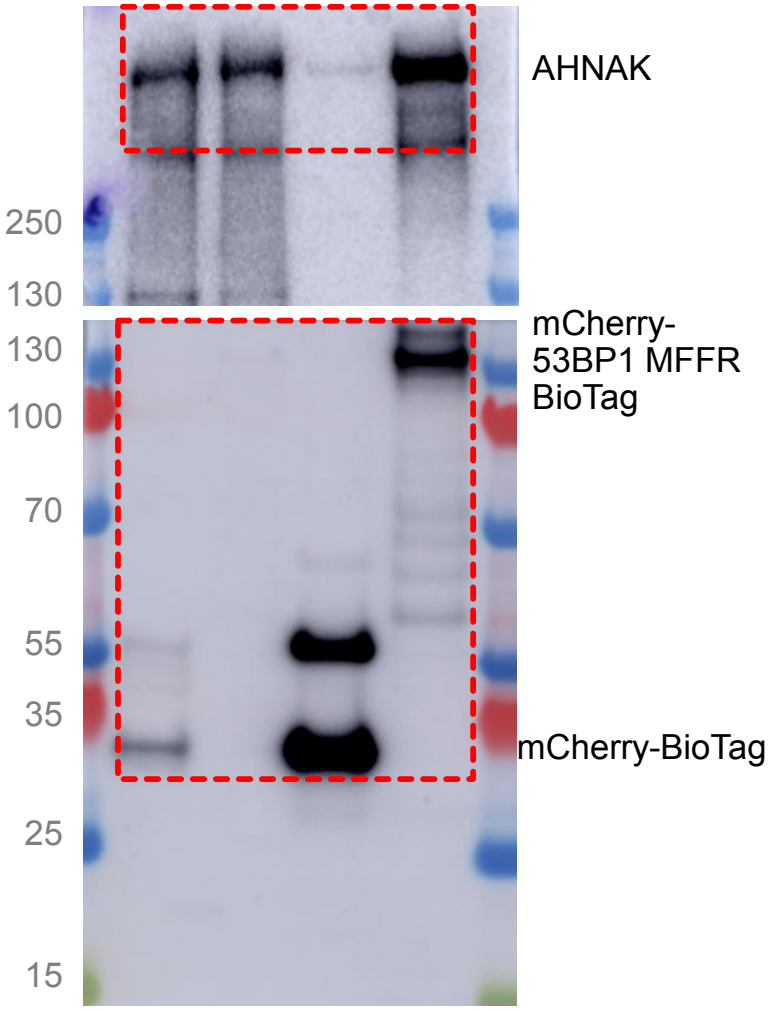

Related to Figure 1D

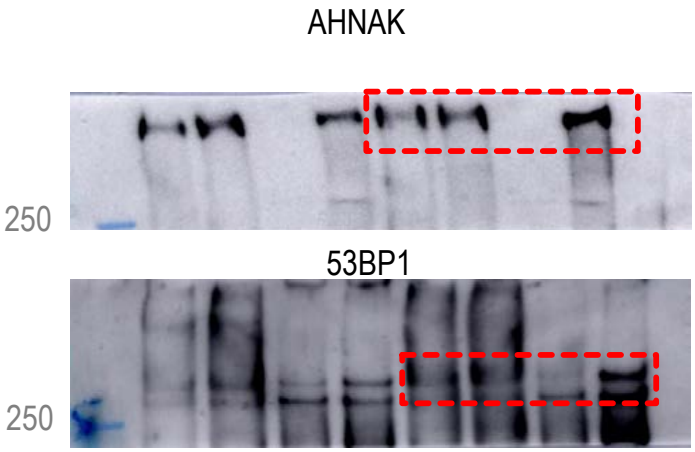

Related to Figure 1F

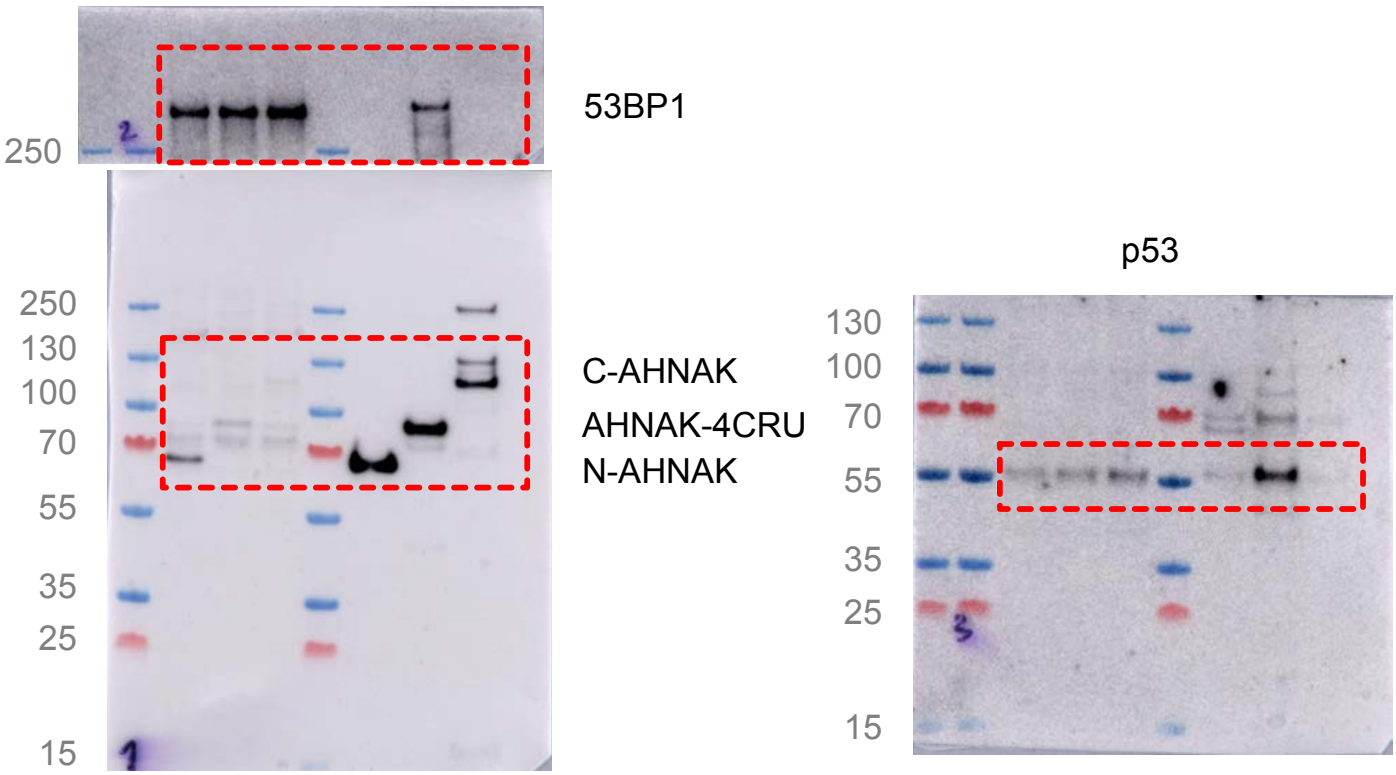

(Related to Figure 1)

Related to Figure 1G

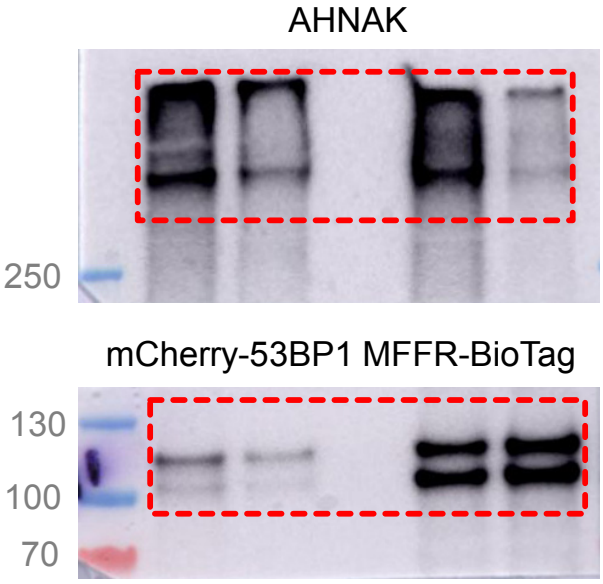

Related to Figure 1H

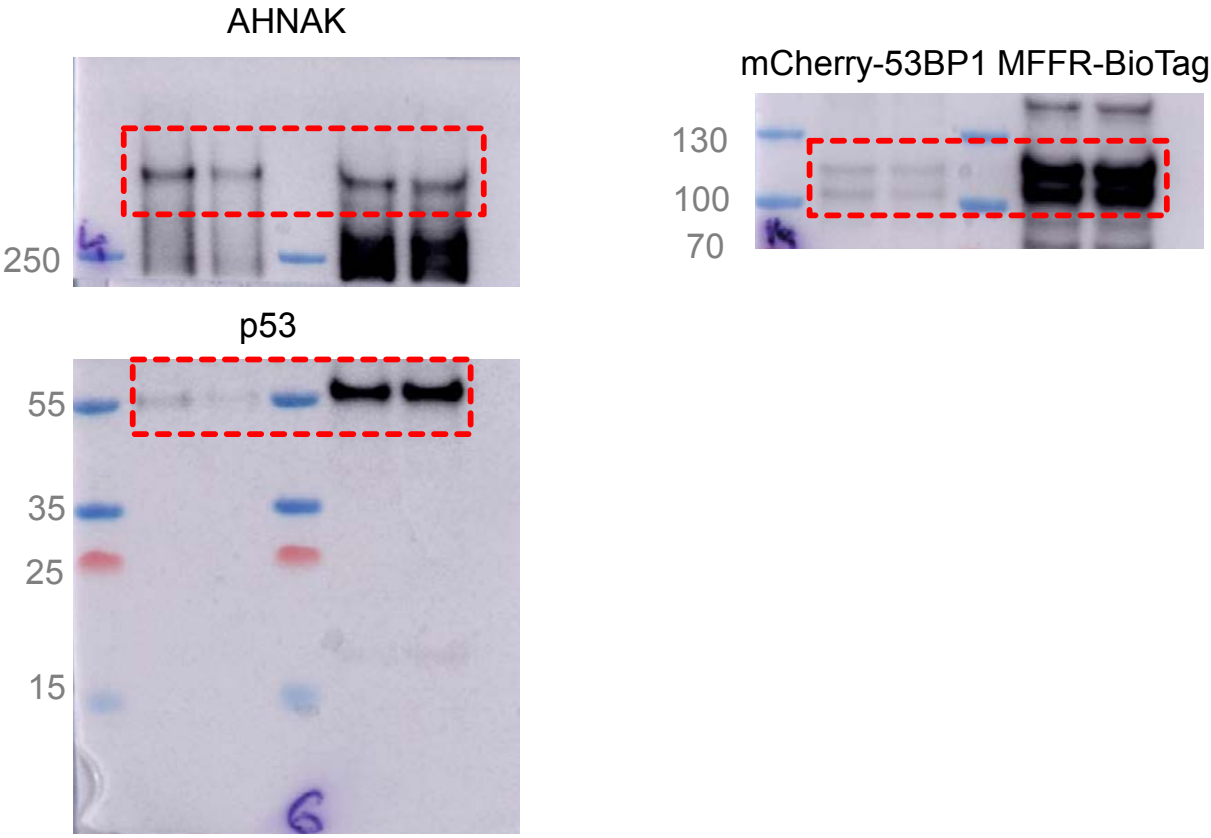

(Related to Figure 1)

Related to Figure 1I

AHNAK

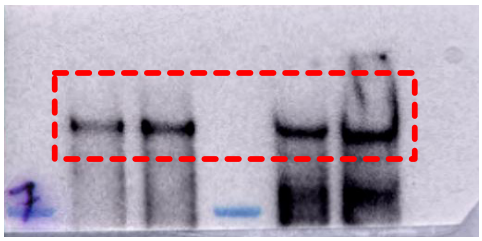

mCherry-53BP1 MFFR-BioTag

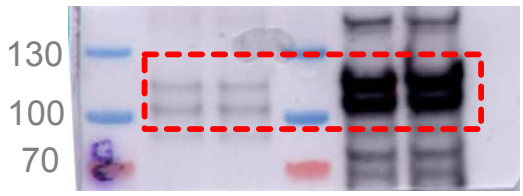

p53

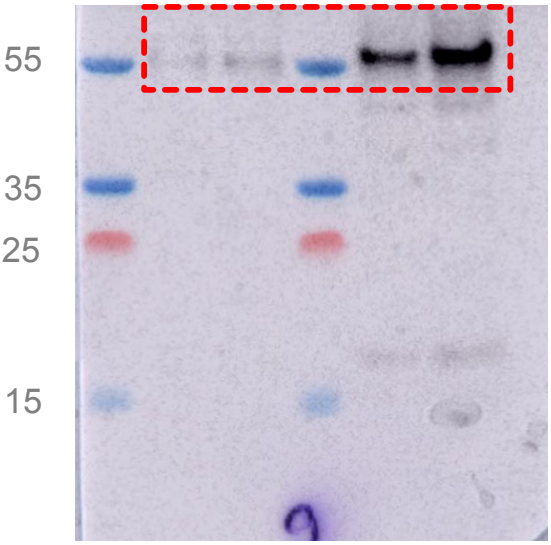

(Related to Figure 1)

Related to Figure1J

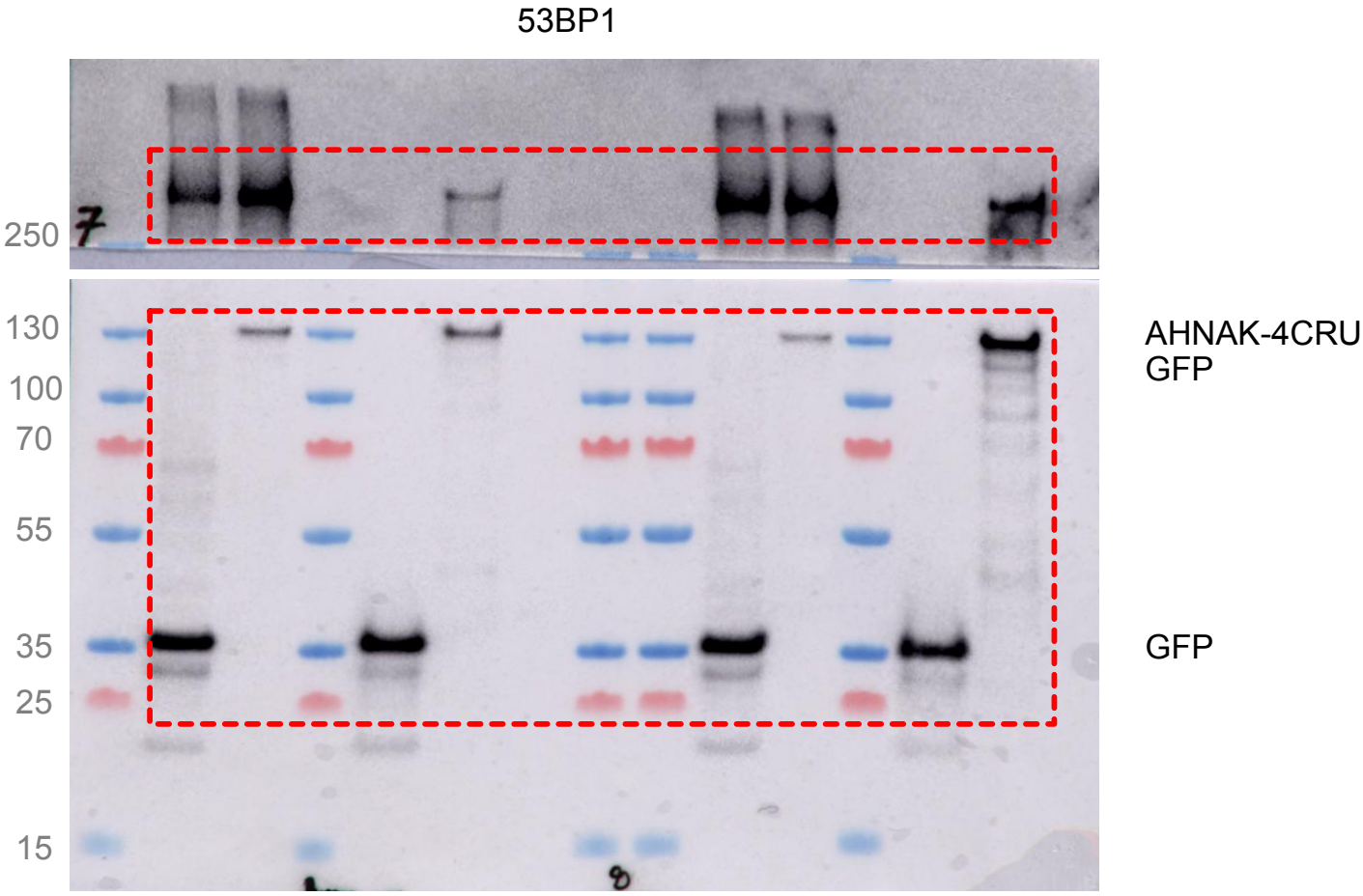

Related to Figure 1K

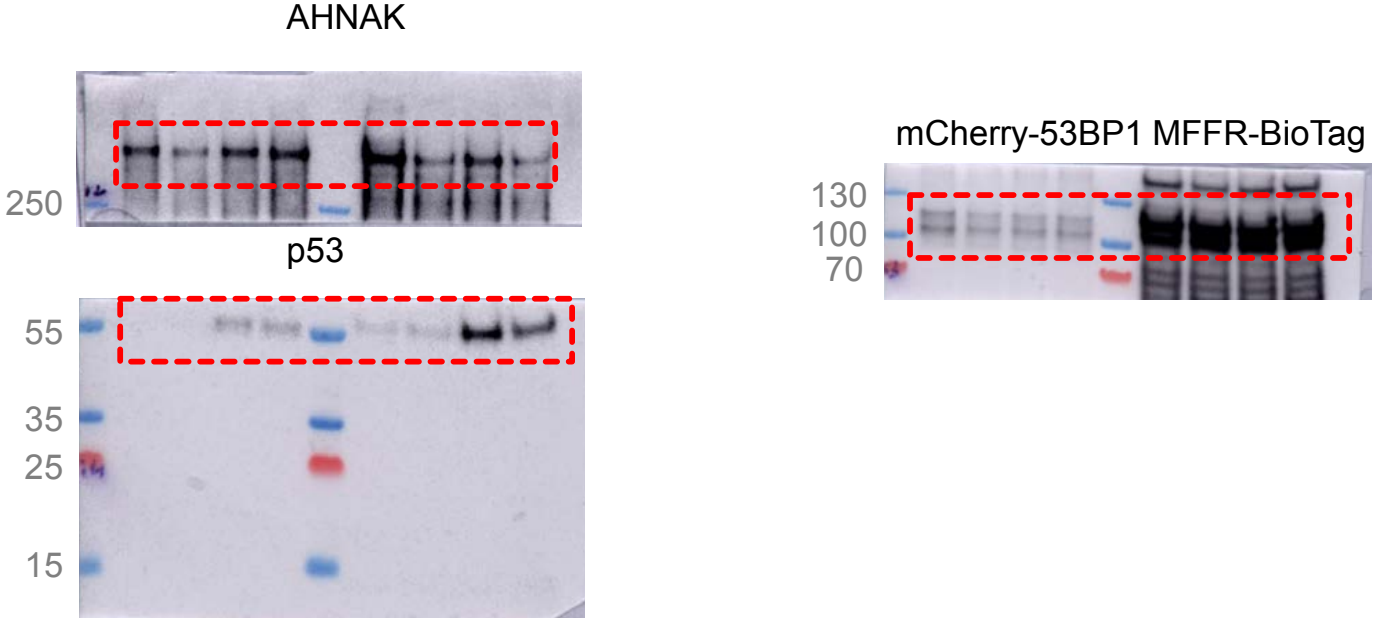

(Related to Figure 2)

Related to Figure 2A

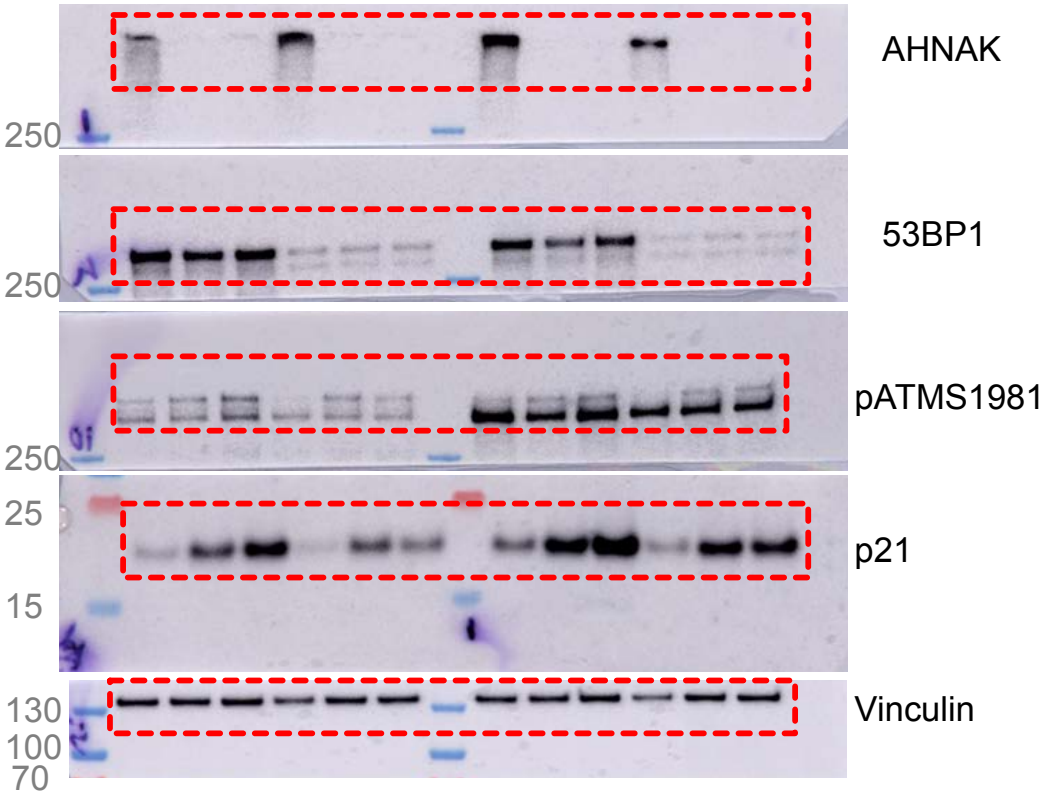

(Related to Figure 2)

Related to Figure 2l

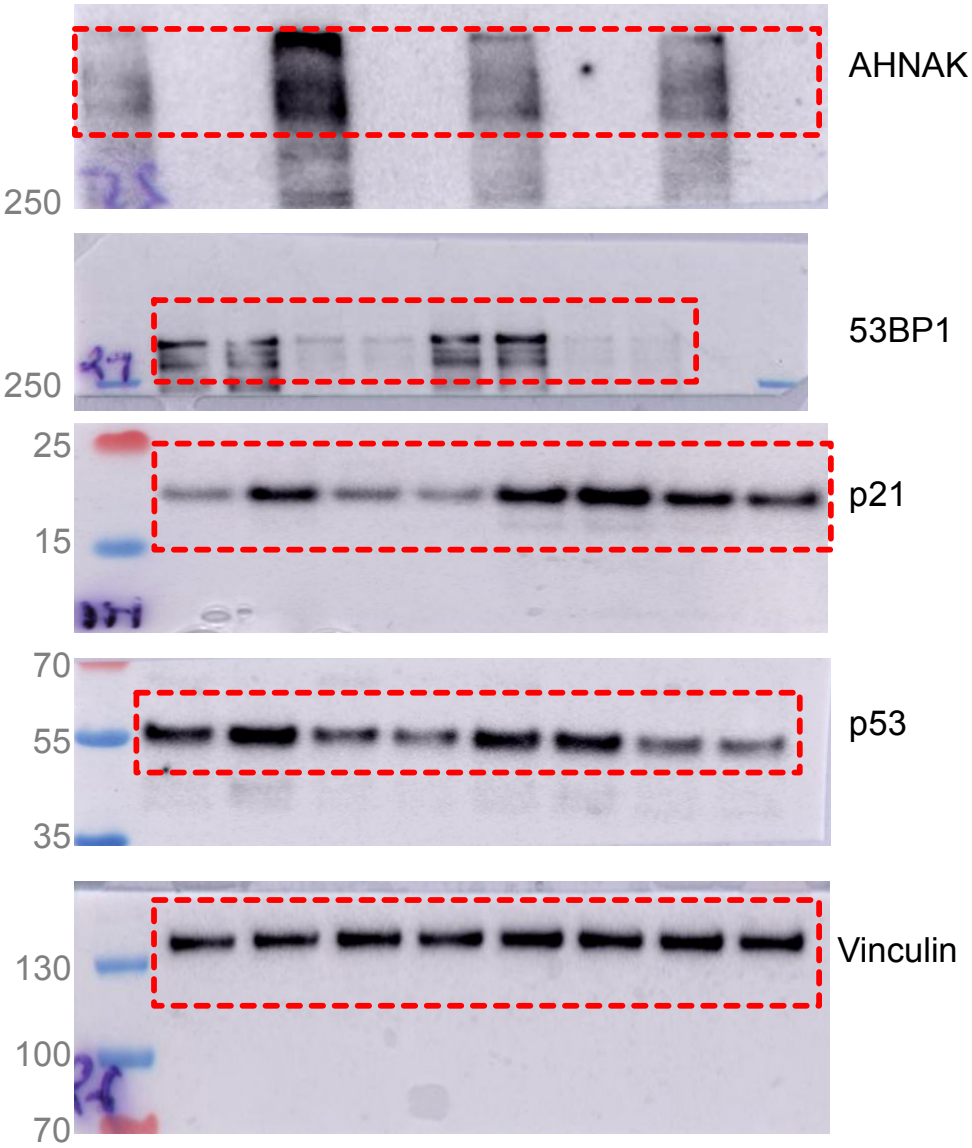

(Related to Figure 2)

Related to Figure 2K

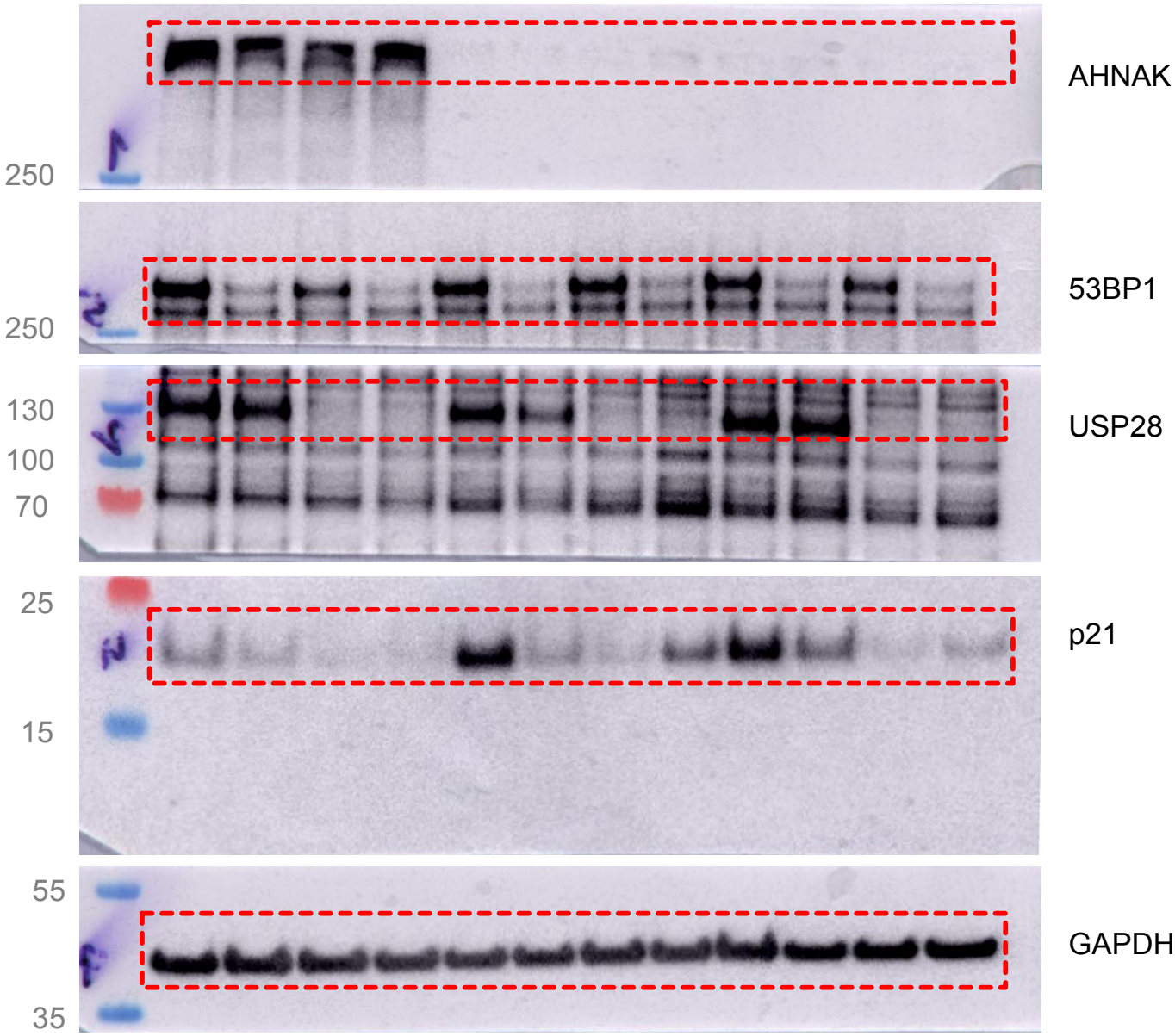

Related to Figure 2L

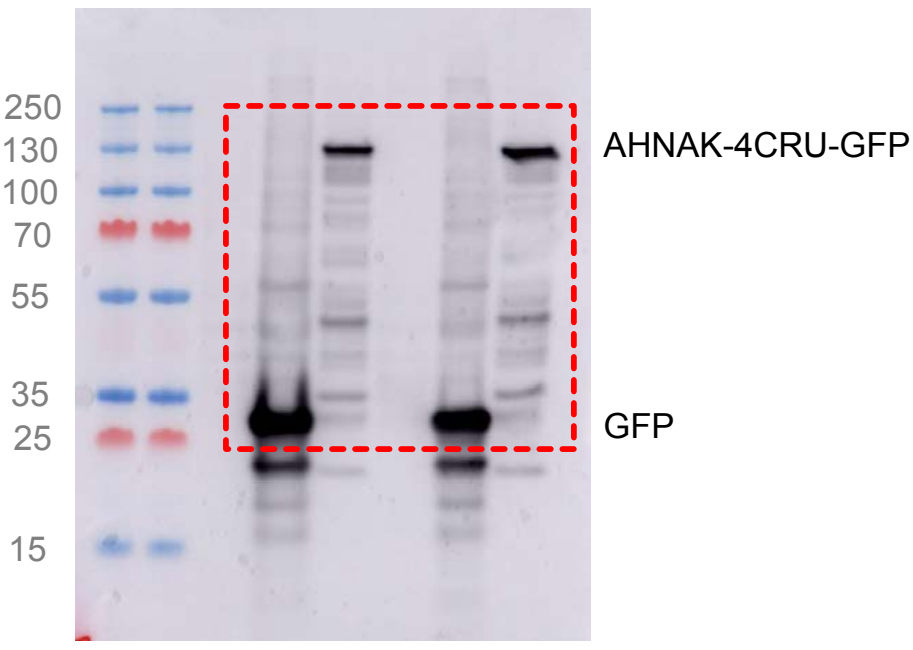

(Related to Figure 2)

Related to Figure 2M

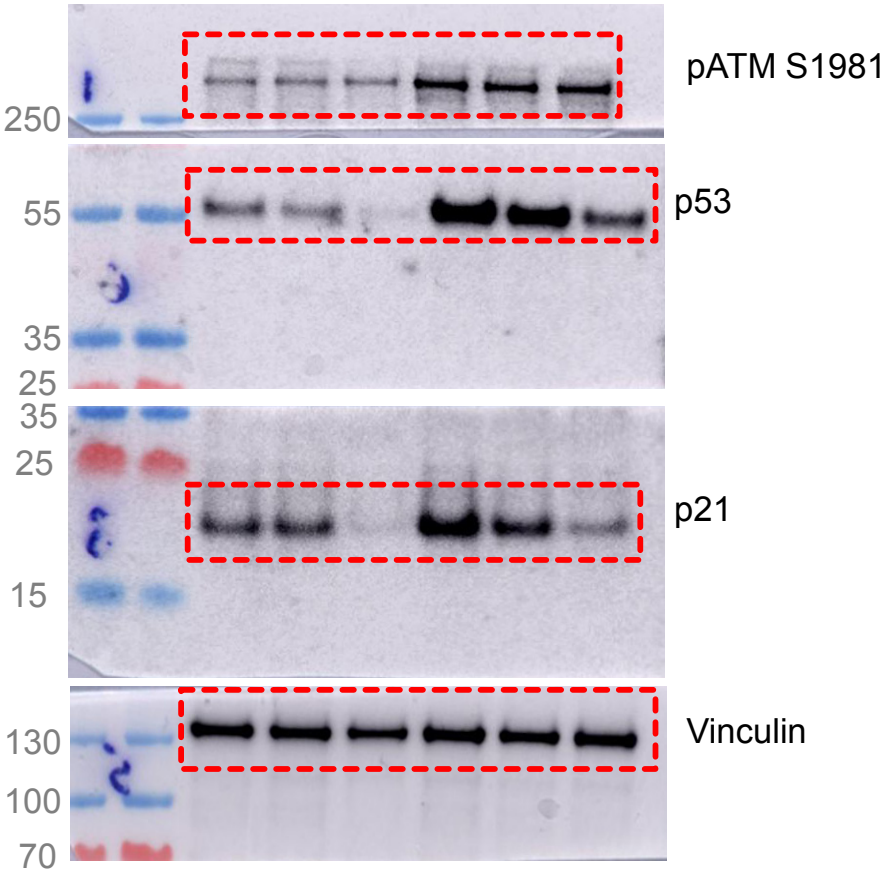

(Related to Figure 4)

Related to Figure 4C

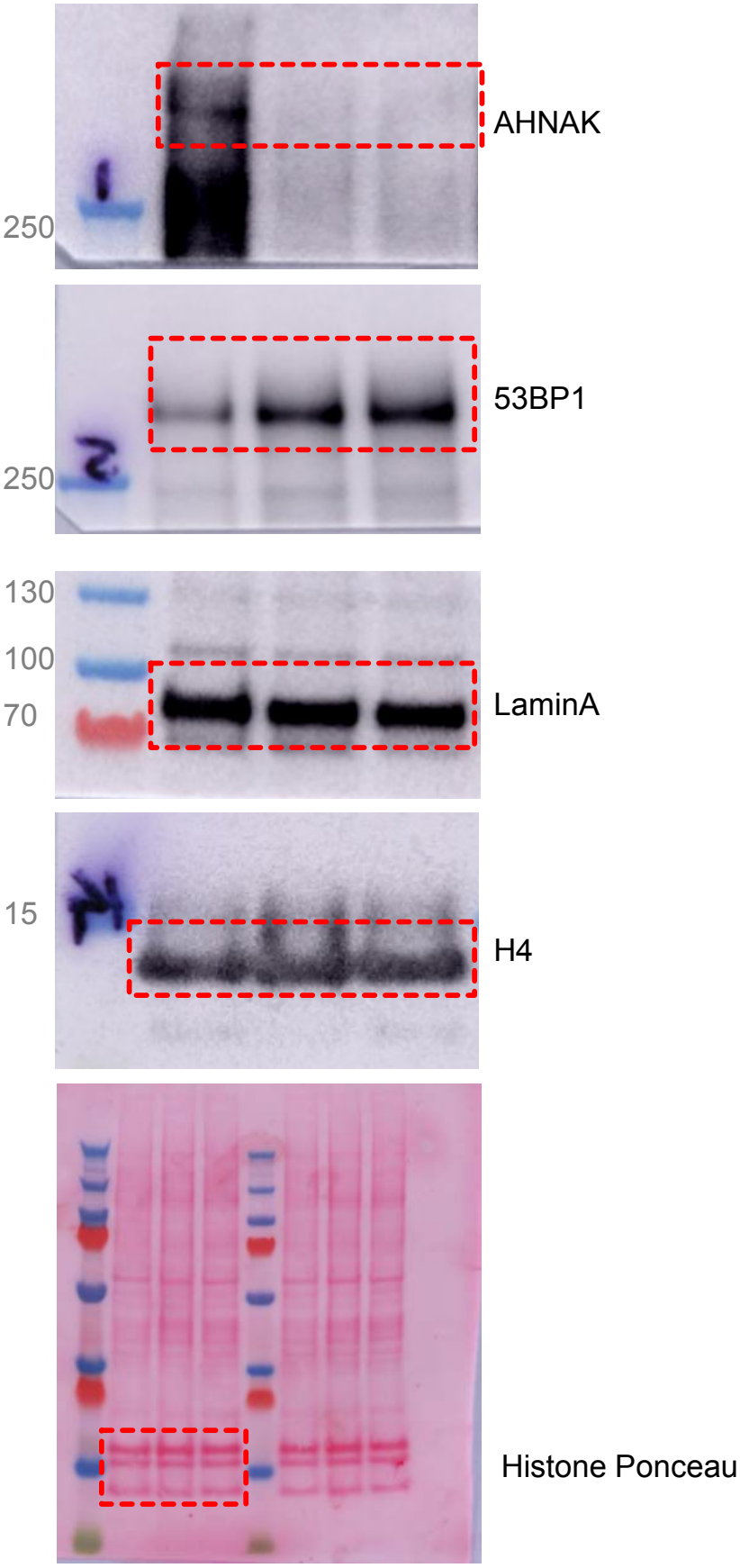

(Related to Figure 4)

Related to Figure 4H

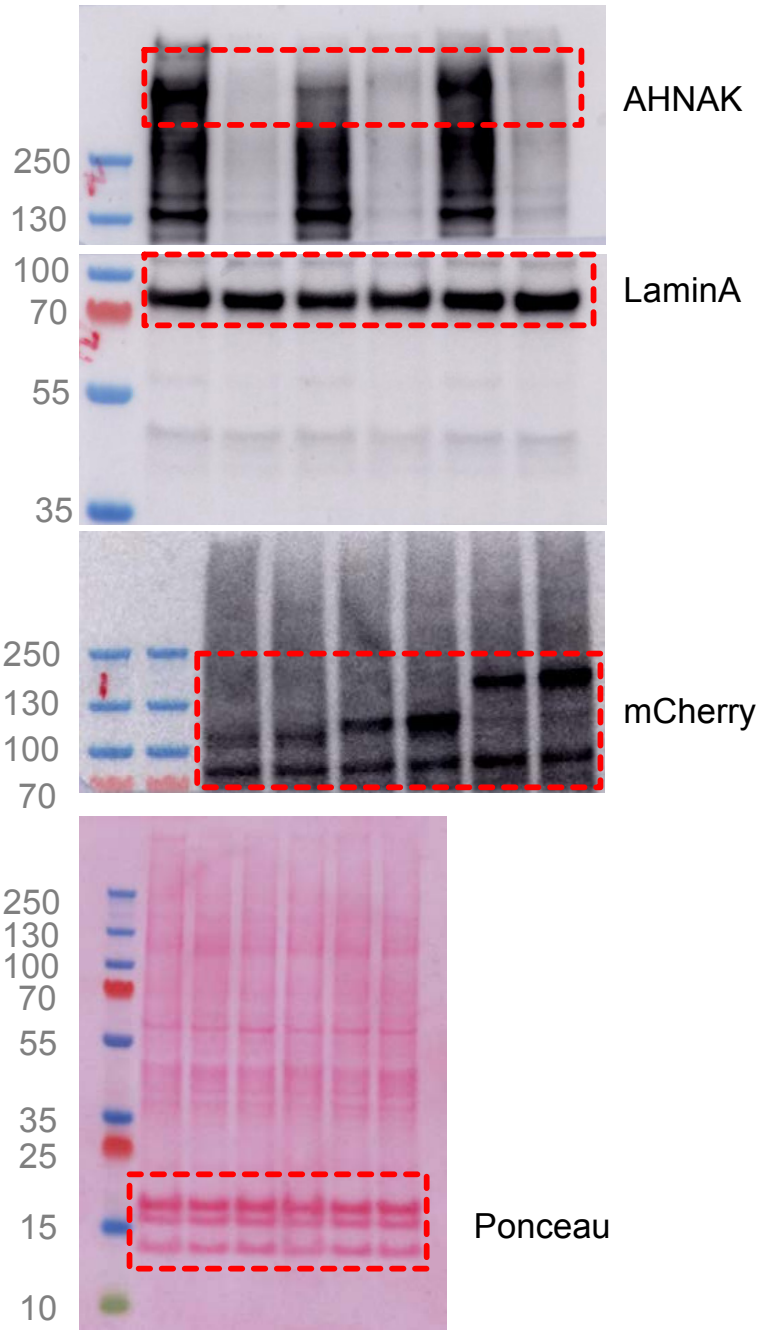

(Related to Figure 4)

Related to Figure 4I

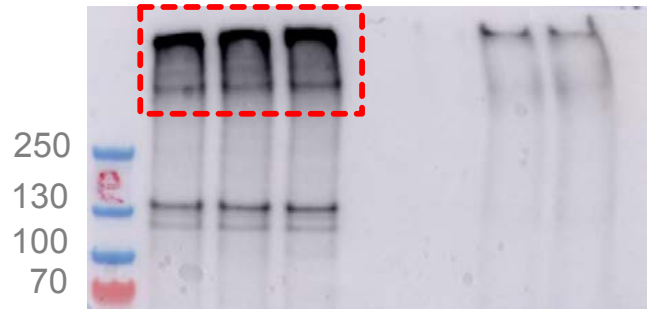

Strip placed on input samples with high exposure

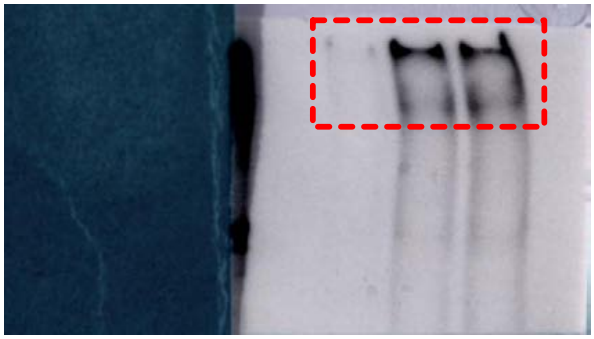

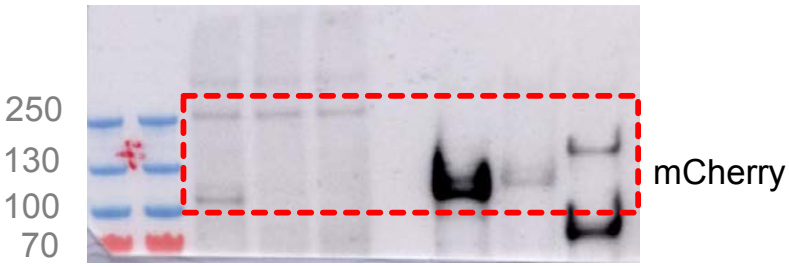

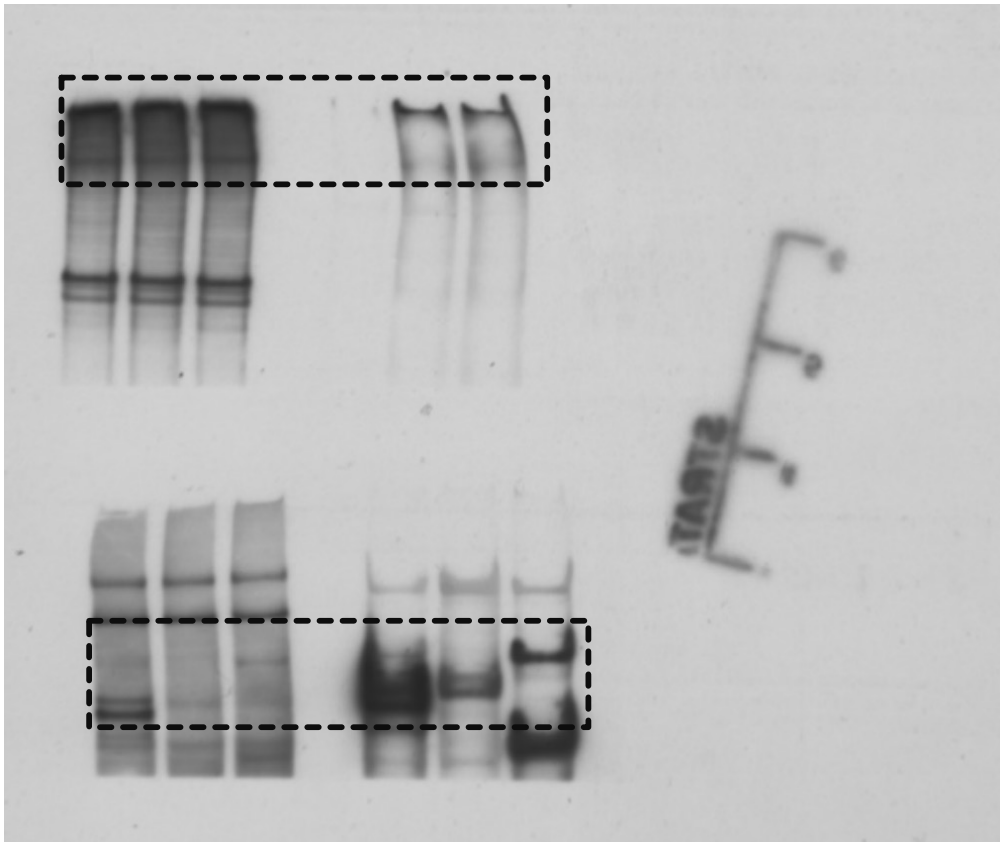

(Related to Figure 5)

Related to Figure 5l

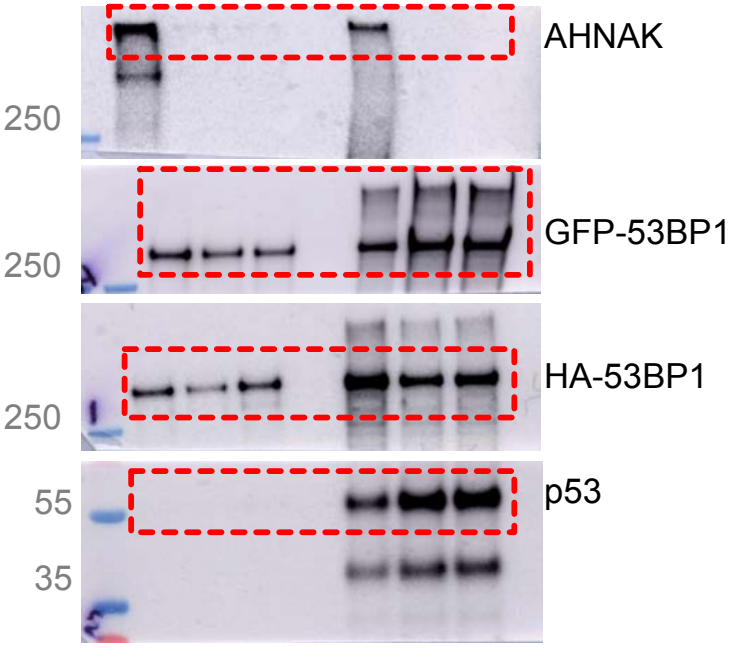

(Related to Figure S1)

Related to Figure S1D

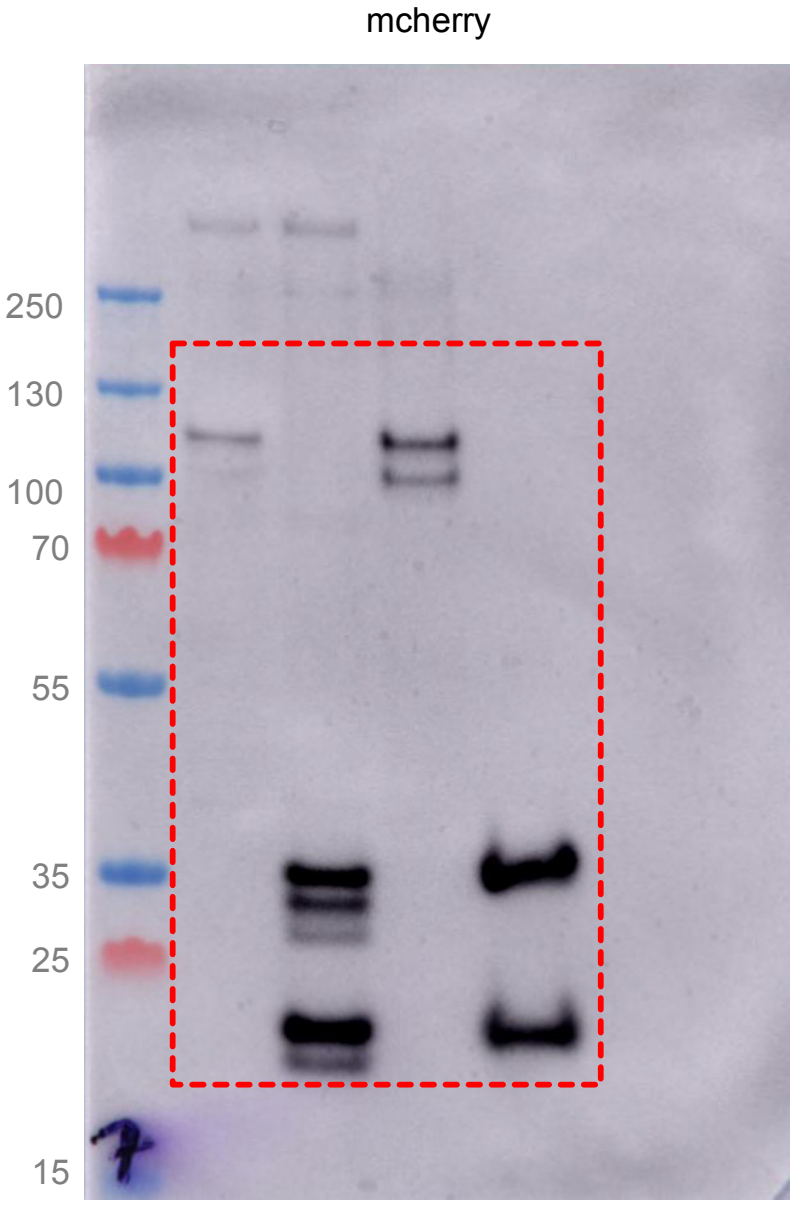

(Related to Figure S1)

Related to Figure S1E

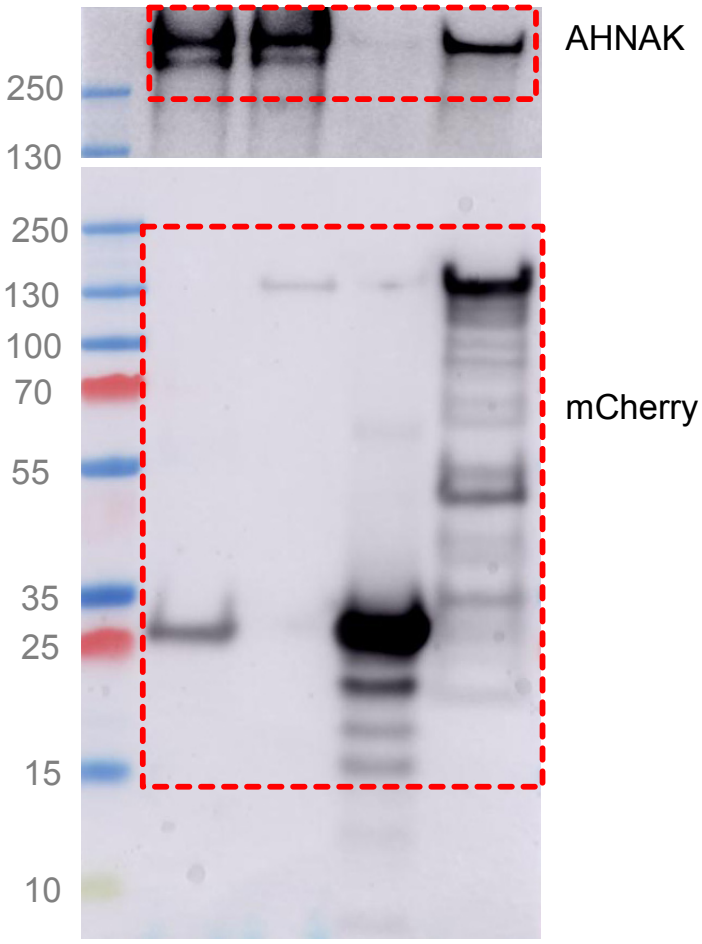

Related to Figure S1F

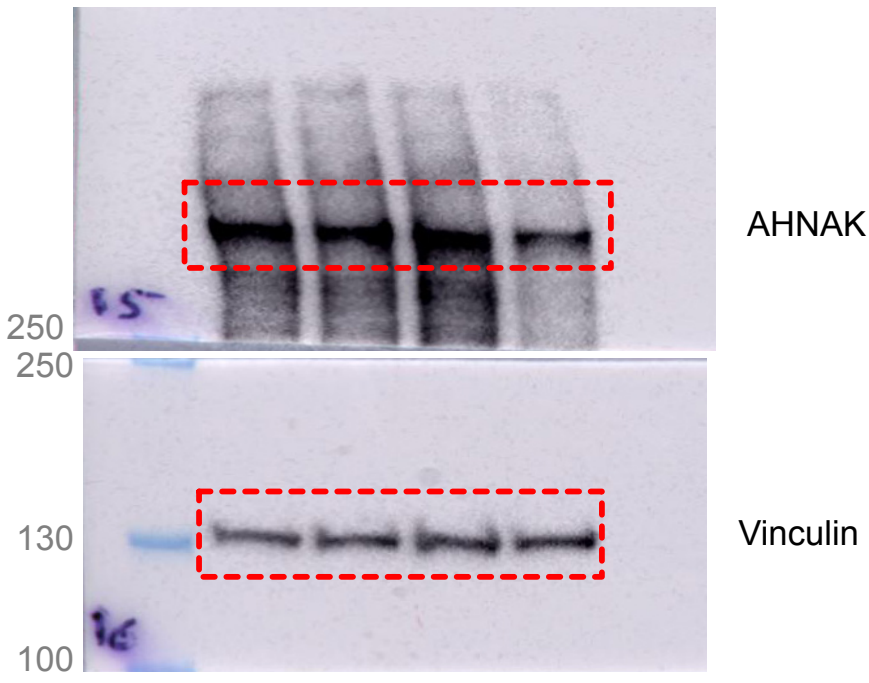

(Related to Figure S1)

Related to Figure S1G

Soluble Fraction

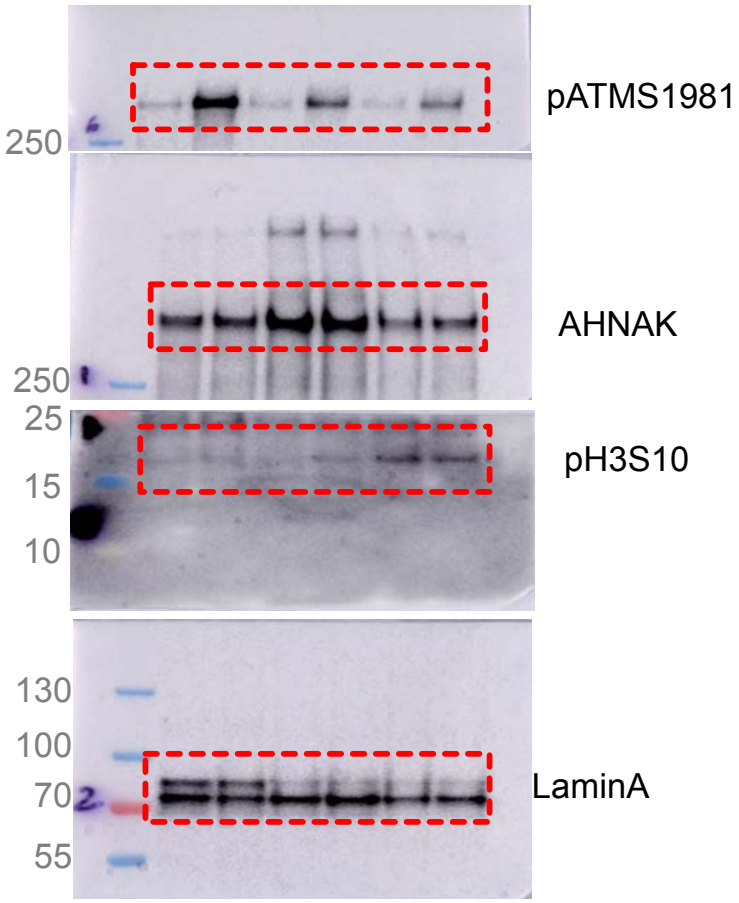

Chromatin Fraction

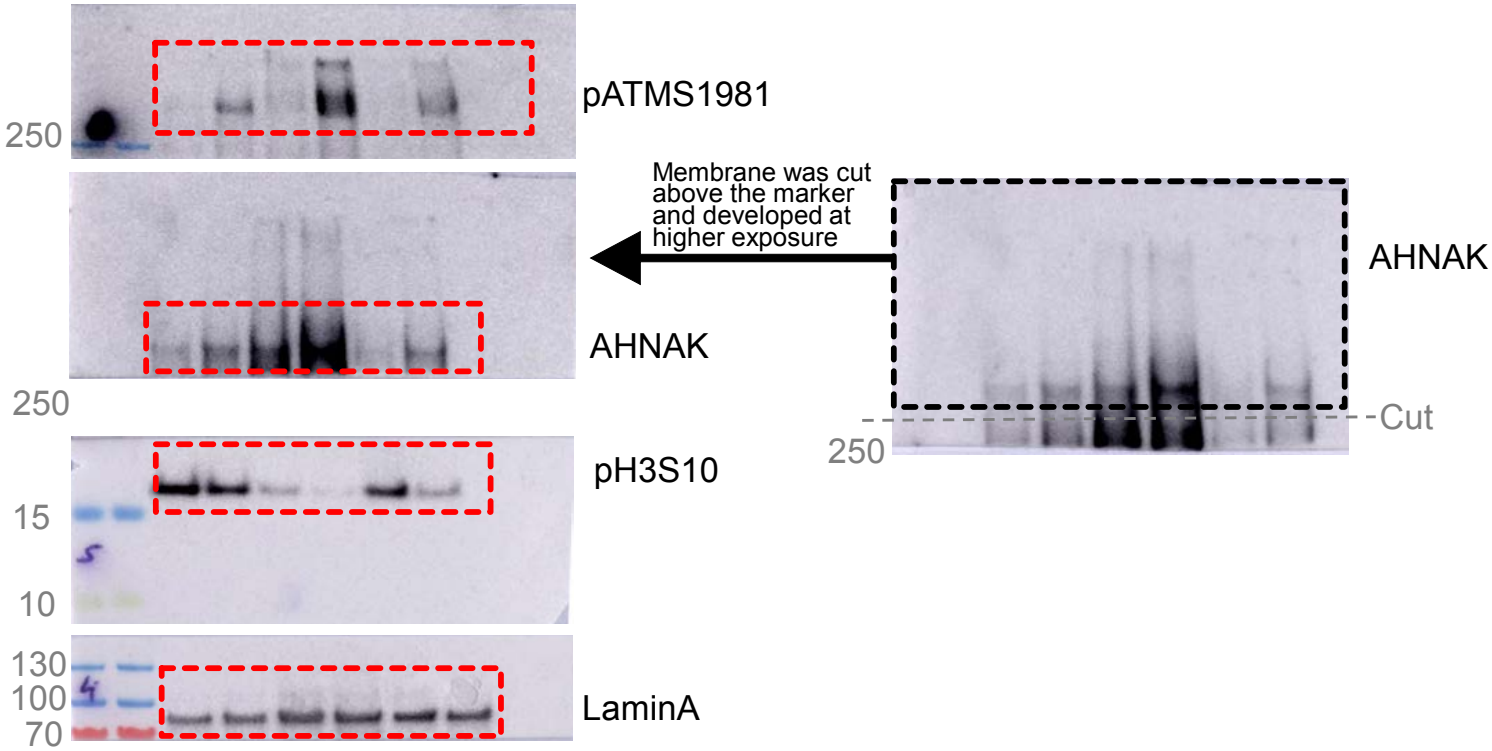

(Related to Figure S2)

Related to Figure S2B

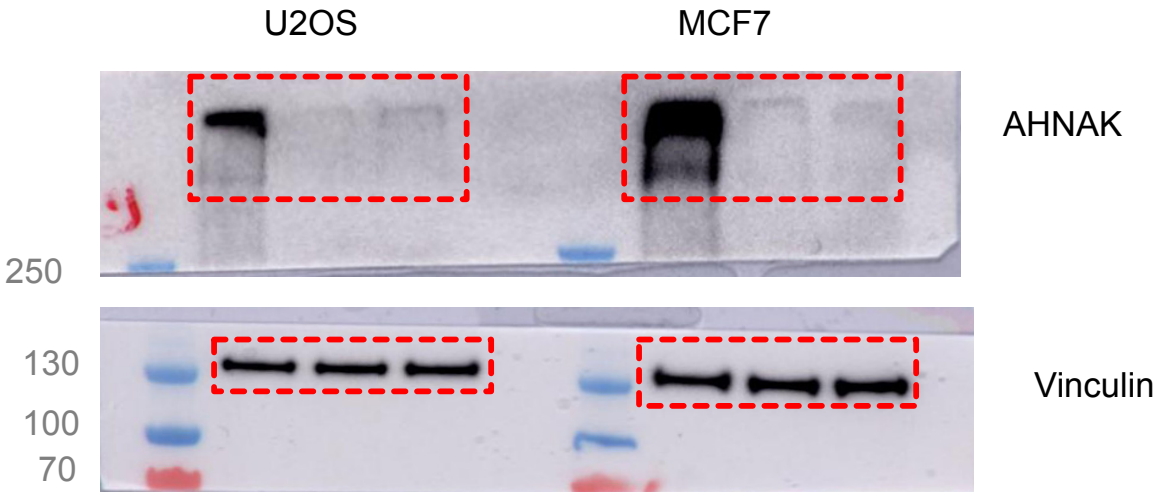

Related to Figure S2D

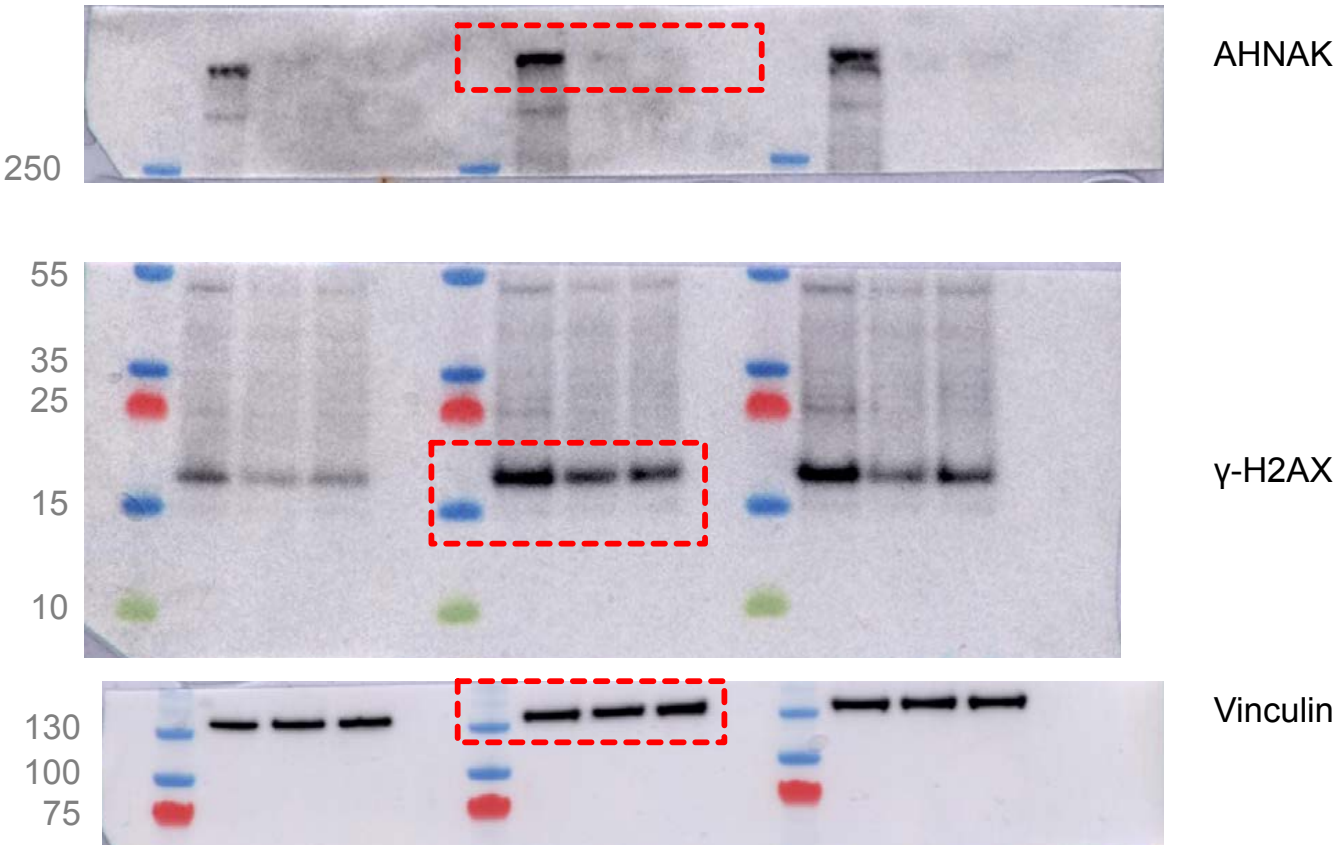

(Related to Figure S2)

Related to Figure S2E

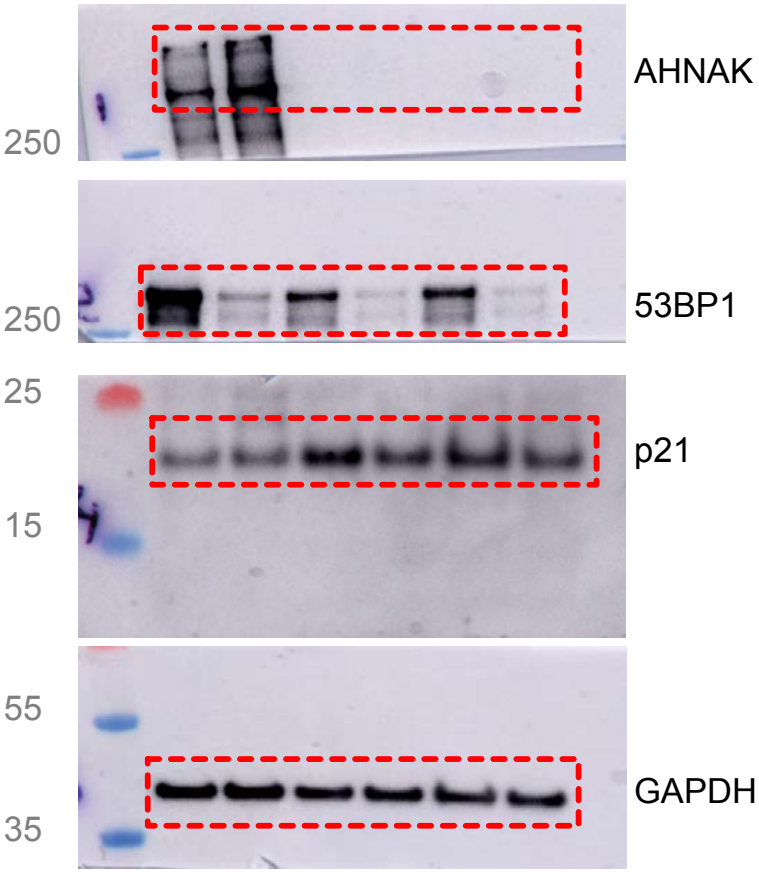

(Related to Figure S2)

Related to Figure S2F

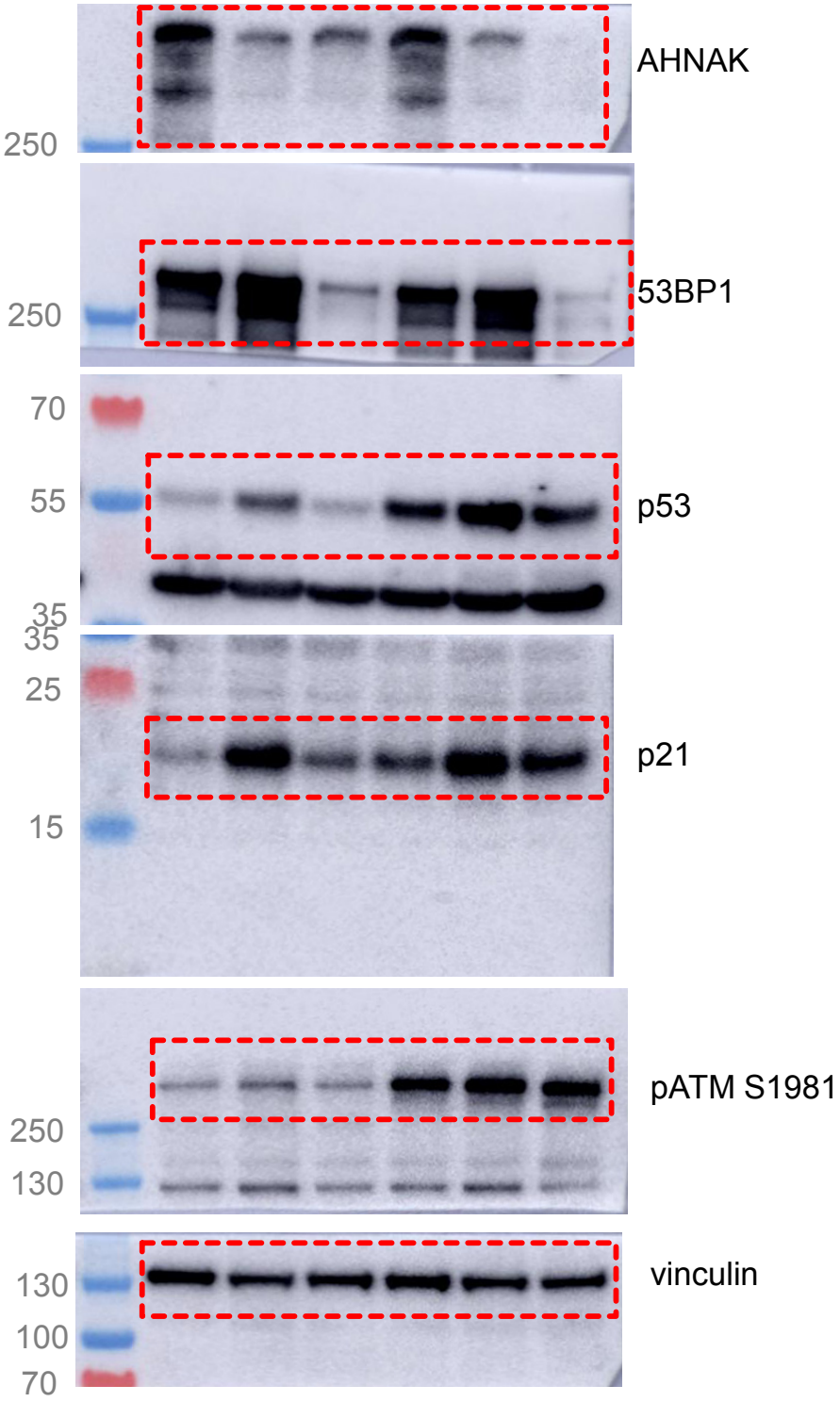

(Related to Figure S2)

Related to Figure S2G

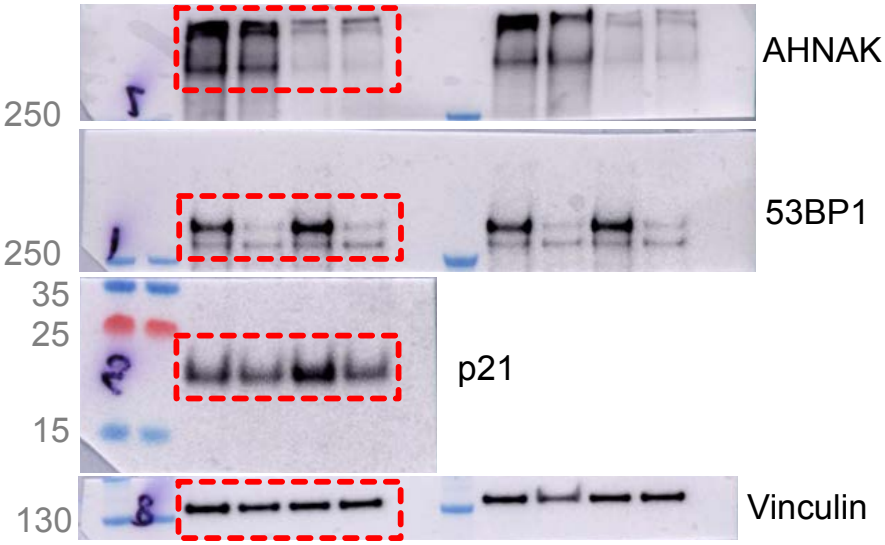

(Related to Figure S3)

Related to Figure S3C

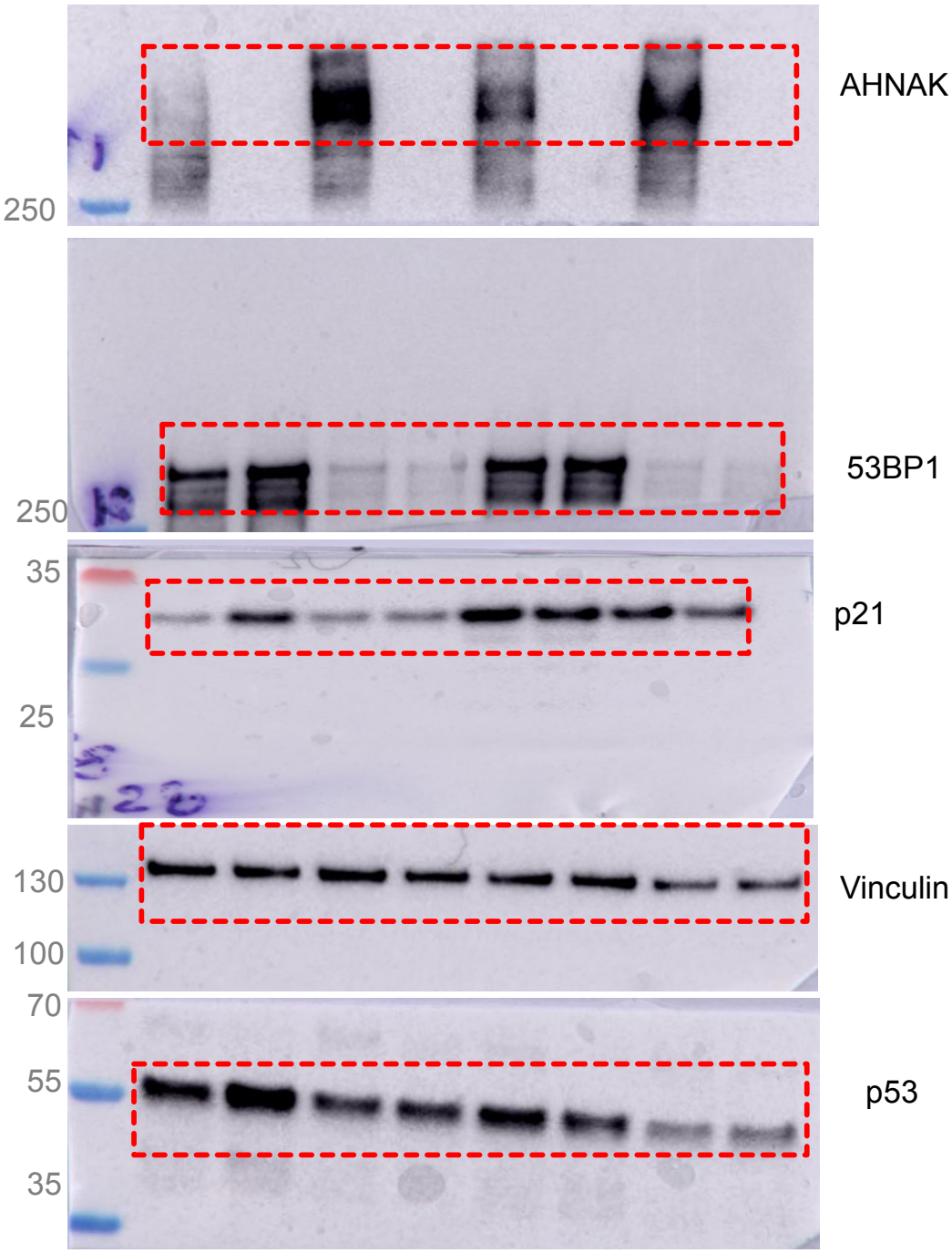

(Related to Figure S3)

Related to Figure S3E

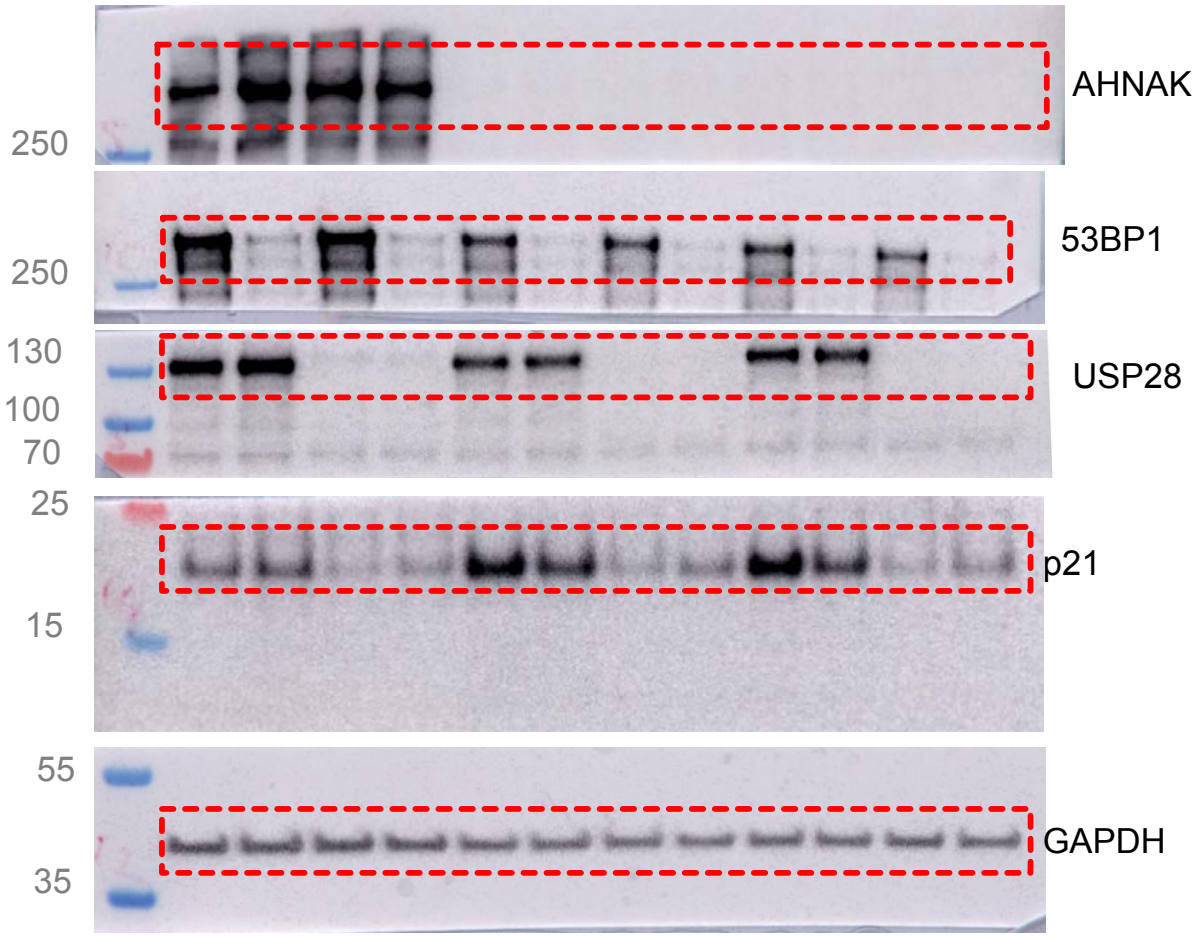

(Related to Figure S5)

Related to Figure S5C

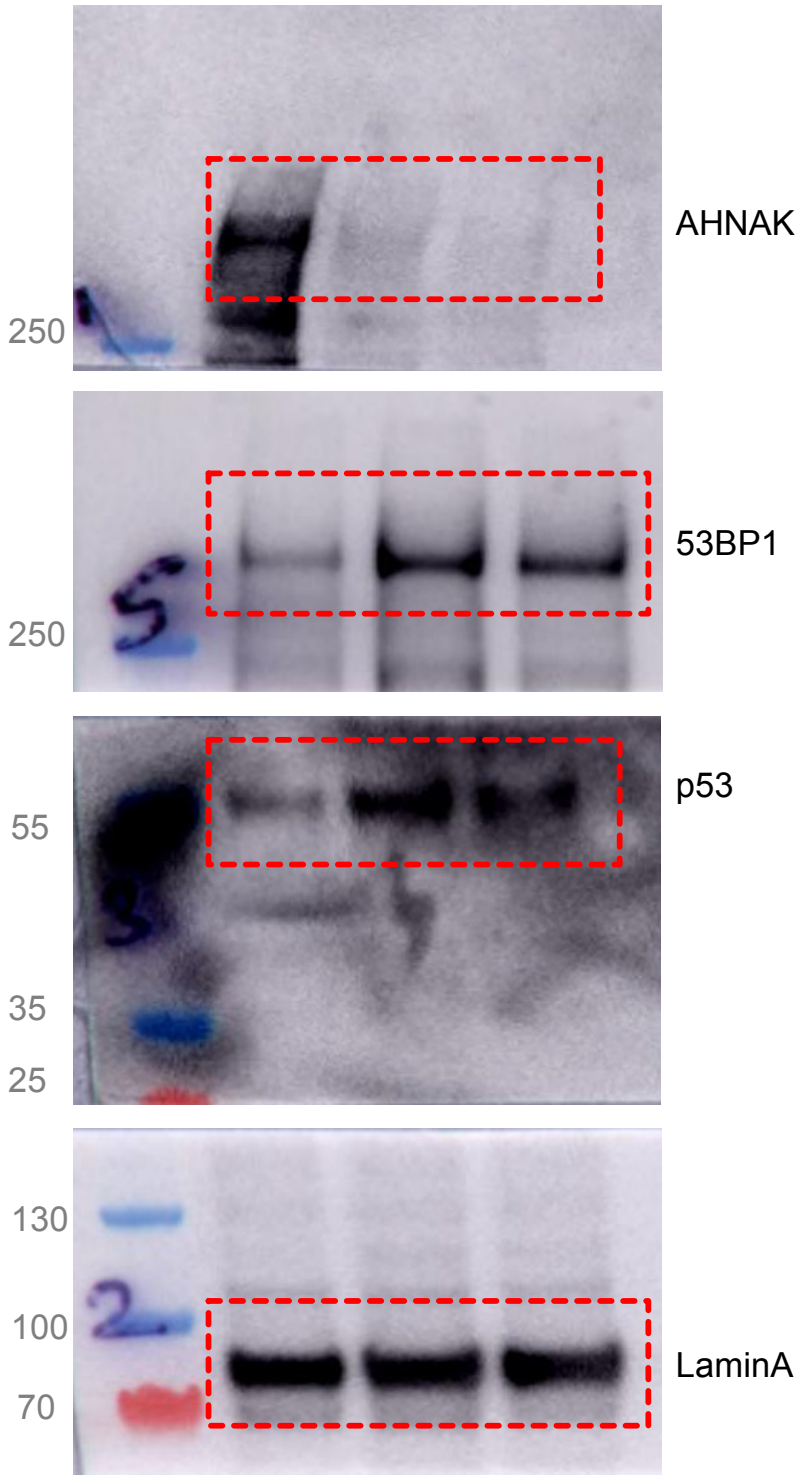

(Related to Figure S5)

Related to Figure S5D

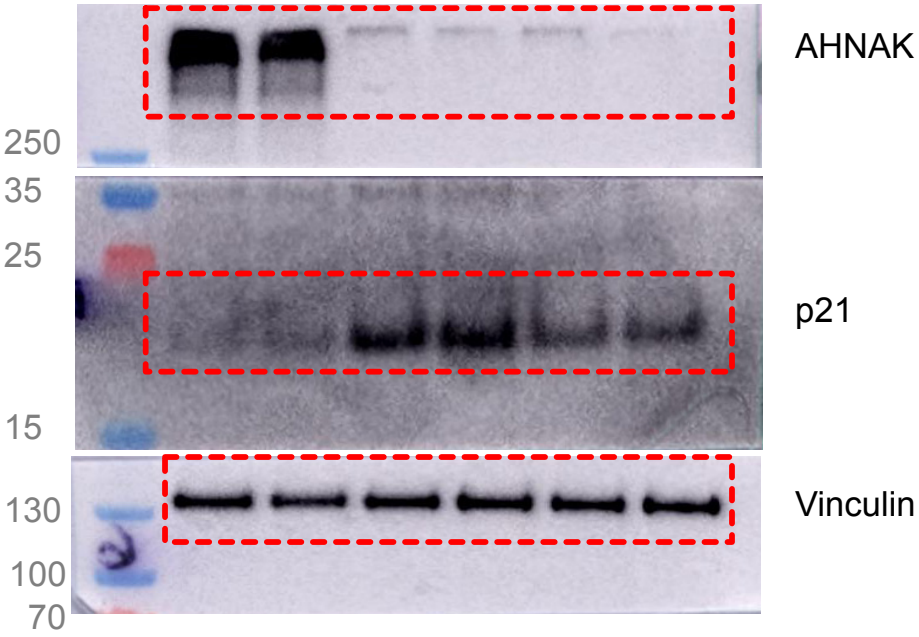

Related to Figure S5G

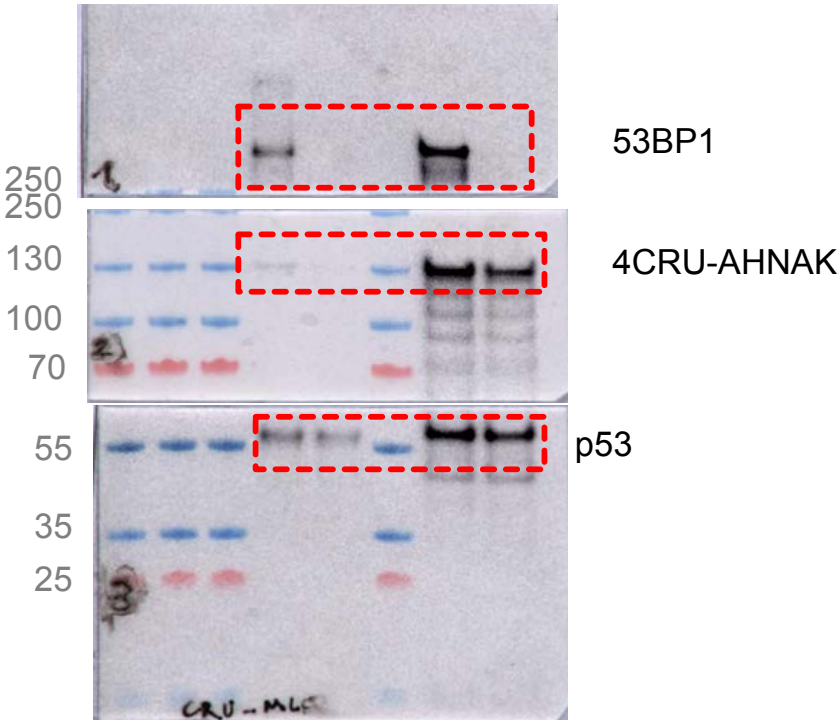

(Related to Figure S5)

Related to Figure S5H